



Title	Preparation of Aromatic Condensation Polymers with Increased Solubility and Gas Permselectivity
Author(s)	Sakaguchi, Yoshimitsu
Citation	大阪大学, 1992, 博士論文
Version Type	VoR
URL	https://doi.org/10.11501/3091084
rights	
Note	

The University of Osaka Institutional Knowledge Archive : OUKA

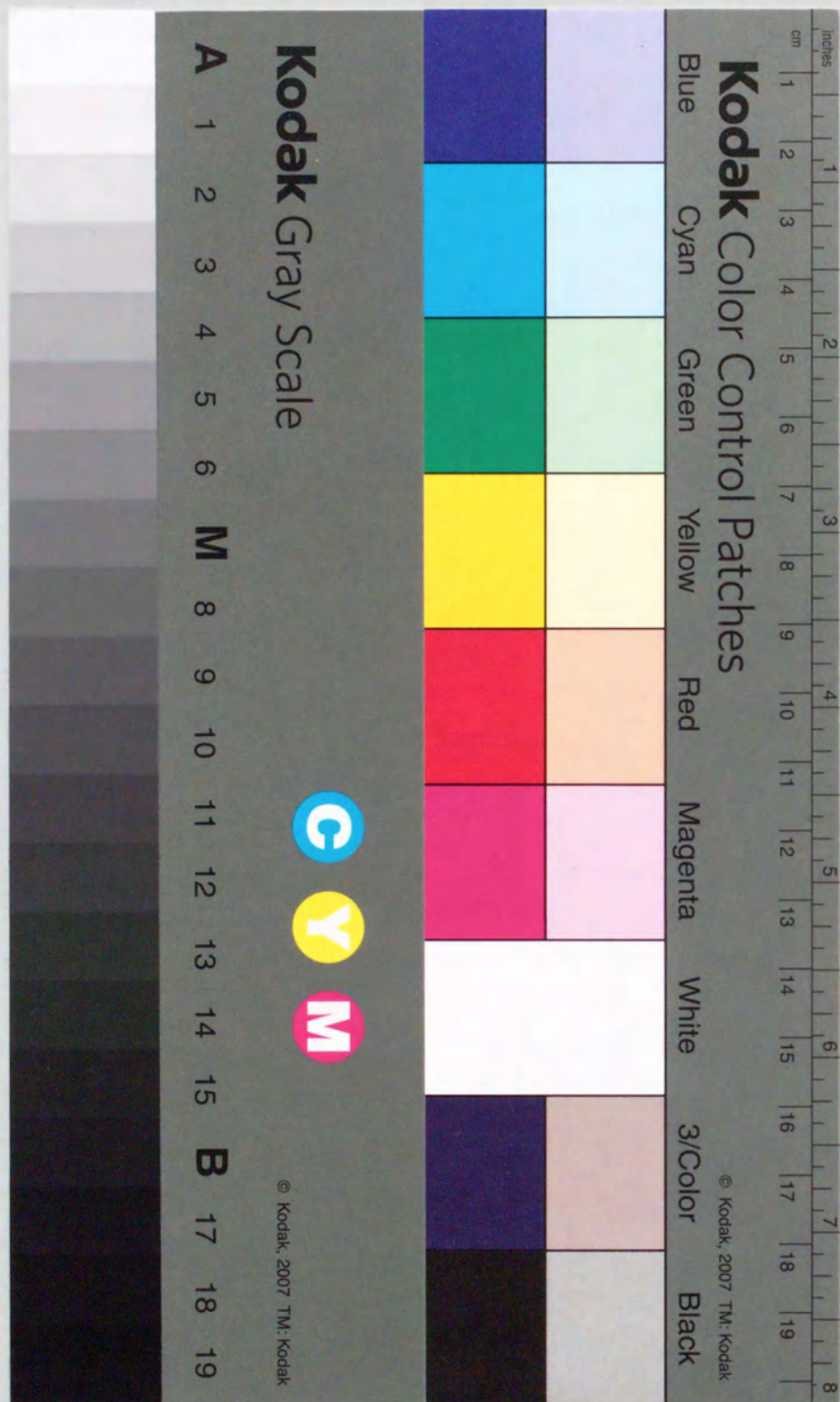
<https://ir.library.osaka-u.ac.jp/>

The University of Osaka

PREPARATION OF AROMATIC CONDENSATION POLYMERS
WITH
INCREASED SOLUBILITY AND GAS PERMSELECTIVITY

by
YOSHIMITSU SAKAGUCHI

Submitted to the Faculty of
Science, Osaka University
September, 1992



①

Preparation of Aromatic Condensation Polymers
with
Increased Solubility and Gas Permselectivity

A Doctoral Thesis
by
Yoshimitsu Sakaguchi

Submitted to the Faculty
of Science, Osaka University

September, 1992

Approval

September, 1992

This thesis is approved as to
style and content by

蒲池 幹治

Member-in-chief

小高 忠男

Member

中村 晃

Member

森島 洋太郎

Member

Acknowledgements

This research except chapter 1 was performed at Toyobo Research Center, Toyobo Co., Ltd. The author is greatly indebted to Dr. Yasuo Kato, Toyobo Co., Ltd., for his cordial guidance and constant encouragements. The research described in chapter 1 was carried out at the Institute of Polymer Science, The University of Akron. He also expresses his sincerest thanks to Professor F.W.Harris for his cordial guidance. The author is deeply indebted to Professor Mikiharu Kamachi at the Department of Macromolecular Science, Faculty of Science, Osaka University for reading the manuscript and providing much kind advice.

The author is grateful to Dr. Hiroyoshi Kamatani, Toyobo Co., Ltd., for his helpful suggestion and encouragements. He expresses his thanks to Mr. Michio Isshi, Managing Director, Mr. Kuniomi Etoh, Director, and Takeo Nishi, Senior General Manager, Toyobo Co., Ltd., for permitting the publication. He also wishes to express his thanks to Messrs. Masaya Tokai and Hiroshi Kawada for their cooperation and discussion. His thanks are due to the members of former Dr. Kato's group, Toyobo Research Center, for their collaboration and useful discussion.

September, 1992

坂口 佳充
Yoshimitsu Sakaguchi

Contents

Introduction	1
References	7
Chapter 1. Synthesis and Characterization of Aromatic Polyamides Derived from New Phenylated Aromatic Diamines	9
1-1. Introduction	10
1-2. Experimental	11
1-3. Results and Discussion	19
1-3-1. Monomer Synthesis	19
1-3-2. Polymerization	22
1-3-3. Characterization	25
1-4. Conclusions	29
References	30
Chapter 2. Synthesis of Poly(ether ketone) by Friedel-Crafts Acylation: Effects of Reaction Conditions	32
2-1. Introduction	33
2-2. Experimental	35
2-3. Results and Discussion	37
2-3-1. Influence of Reaction Conditions on PEK Polymerization	37
2-3-2. Polymerization Behavior in the Polymer Precipitate	43
2-4. Conclusions	48
References	49

Chapter 3. Synthesis of Polyimide and Poly(imide-benzoxazole) in Polyphosphoric Acid	51
3-1. Introduction	52
3-2. Experimental	53
3-3. Results and Discussion	58
3-3-1. Model Reaction in PPA	58
3-3-2. Synthesis of Polyimide in PPA	61
3-3-3. Synthesis of Poly(imide-benzoxazole) in PPA	64
3-4. Conclusions	67
References	68
Chapter 4. Polymer Structure and Gas Permeability of Poly(sulfone-amide) Membranes: Catenation Effect	70
4-1. Introduction	71
4-2. Experimental	72
4-3. Results and Discussion	76
4-3-1. Preparation and Properties of Poly(sulfone-amide)s	77
4-3-2. Gas Permeability of Poly(sulfone-amide) Copolymers	79
4-4. Conclusions	84
References	85
Chapter 5. Polymer Structure and Gas Permeability of Poly(sulfone-amide) Membranes: Effect of Amide-Linkage Concentration	86
5-1. Introduction	87
5-2. Experimental	88

5-3. Results and Discussion	89
5-3-1. Gas Permeability of Poly(sulfone-amide) Copolymers Derived from 4SED and Phenylenediamines	89
5-3-2. Gas Permeability of Poly(sulfone-amide) Copolymers Derived from 3DDS and Phenylenediamines	96
5-4. Conclusions	103
References	104
Chapter 6. Change of Gas Permeability and Membrane Structure of Poly(sulfone-amide)s in the Process of Solvent Removal	105
6-1. Introduction	106
6-2. Experimental	107
6-3. Results and Discussion	109
6-3-1. Thermal Treatment of As-cast Membrane	109
6-3-2. Thermal treatment of Extracted Membrane	120
6-4. Conclusions	126
References	127
Chapter 7. Effects of Polymer Structure and Thermal Treatment on Gas Permeability of Poly-(ether ketone)s	128
7-1. Introduction	129
7-2. Experimental	131
7-3. Results and Discussion	134
7-3-1. Polymer Structure and Gas Permeability of Poly(ether ketone)s	134
7-3-2. Gas Permeability of the Thermally Treated Films	140

7-4. Conclusions	145
References	146
Summary	147
Conclusions	149
List of Publications	151

Introduction

Aromatic condensation polymers have phenylene rings which provide rigidity and thermal stability in the main chain, and they have potential for the preparation of high performance materials. Polyimides, aramids, polyarylates, and poly(arylene ether)s are well-known examples of high performance polymers owing to their superior thermal stability, chemical resistance, and mechanical behavior.¹ However, these properties also make it difficult to process and fabricate the polymers. From these points of view, a number of researches have been reported to enhance the solubility or fusibility of aromatic polymers.²⁻¹⁶

Aromatic polyamides have been commercialized as materials for films, fibers and other applications with high thermal stability and mechanical properties. Especially, a high-strength and high-modulus fiber was made from poly(paraphenylene terephthalamide). As this polymer did not dissolve in any organic solvents, the spinning was possible only from a solution in concentrated sulfuric acid.¹⁷ To increase the limited solubility, modifications of the polymer structure have been studied by introducing flexible linkages in the polymer backbone²⁻⁶ and/or bulky substituents as the side chains.⁷⁻⁹

Among poly(ether ketone)s, poly(ether ether ketone) is well-known as a semi-crystalline engineering thermoplastics.^{18,19} Although it shows outstanding heat- and chemical-resistance, a considerably high temperature is necessary to mold this resin. Therefore, various poly(ether ketone)s of modified structures have been synthesized to control their glass transition and melting temperatures.¹⁰⁻¹⁴

Polyimides are one of the highest heat-resistant and chemically stable polymers, being used as materials for films and moldings.²⁰ As polyimides are generally infusible and insoluble, they are processed from the soluble precursors, poly(amic acid)s, which are then converted to the imide structure. The imidization process sometimes leads to void formation in the product and shows difficulties in complete cyclization. Syntheses of processable polyimides which are soluble or fusible have been studied actively based on these backgrounds.¹⁵

In order to increase the processability of aromatic condensation polymers, particularly to increase their solubility, basic research from the following points is meaningful: (1) to understand the relationships between polymer structure and solubility by changing systematically the polymer structure, (2) to clarify optimum polymerization conditions for potentially soluble poly-

mers which have difficulties in the polymerization, and (3) to find out a new solvent in which homogeneous polymerization is possible.

Gas separation membrane is considered as one of the promising applications of aromatic condensation polymers. However, low solubility of these polymers has sometimes made it difficult to prepare the membrane. If soluble aromatic condensation polymers are prepared, they are expected to give a membrane suitable for the gas separation membrane. In this research, several soluble polymers were prepared successfully. Therefore, the membranes were made by using these polymers and evaluation of the relationships between gas permeability and polymer structure were investigated.

In general, gas permeation through a polymer membrane is explained in terms of solubility and diffusivity of a gas molecule.²¹⁻²³ In the separation of small gas molecules such as hydrogen and helium from larger molecules such as carbon monoxide and nitrogen, permselectivity is mainly affected by the diffusivity difference, because differences in the solubility of gases are usually small for many polymers.²⁴ Amorphous aromatic polymers have advantages for this type of separation because they have relatively rigid structures and stable chain-packing characteristics.²⁵ Although there are many

reports discussing the relationships between polymer structure and gas permeability, most of them deal with the systems which contain several factors such as different linkages and substituents in the polymer structure. Therefore, a systematic research on gas permeation properties of a series of well-defined aromatic copolymers is a very attractive way to obtain basic information on the molecular design for preparing gas separation membranes.

This thesis consists of seven chapters. Chapters 1 through 3 are concerned with the preparation of soluble aromatic condensation polymers: aromatic polyamides, poly(ether ketone), and polyimides. Chapters 4 through 7 are concerned with gas permeabilities of aromatic polyamides and poly(ether ketone)s.

Chapter 1 describes the relationship between the polymer structure of aromatic polyamides and their solubility in organic solvents. In order to increase the solubility of aromatic polyamides without losing their thermal stability, the introduction of bulky aromatic substituents is one of the best ways.¹⁶ New two series of aromatic diamines containing phenyl substituents were thus synthesized, and allowed to polymerize with aromatic diacid chlorides to afford new soluble aromatic polyamides.

In chapter 2, mechanistic aspects of the formation of poly(ether ketone) by Friedel-Crafts acylation was investigated. The preparation of poly(ether ketone)s via this method is convenient in laboratory scale and able to give varieties of the polymers including potentially soluble ones. However, details of the effects of polymerization conditions have not been reported so far. The polymerization behavior was studied in order to find the optimum conditions to afford high molecular weight polymers.

In chapter 3, the preparation of polyimides in polyphosphoric acid was discussed. In order to obtain processable polyimides, modifications of polymer structures have been performed so far by introducing flexible linkages into the polymer backbone or bulky substituents as the side chains.¹⁵ However, if a new solvent for the preparation of polyimides to give a homogeneous solution is found out, the polyimides which have been reported to be unprocessable would be processable. In this research, polyphosphoric acid was found to be an effective medium for the preparation of polyimides.

In chapters 4 and 5, gas permeations of H_2 and CO through aromatic polyamide membranes containing sulfone linkages in the backbone [these polymers are called poly(sulfone-amide)] were studied. Series of copolymers

with different ratios of *para*- and *meta*-phenylene groups or amide contents in the backbone were prepared, and gas permeabilities of these copolymers were systematically investigated.

Chapter 6 concerns with the relationships between the process of membrane formation and gas permeability of the poly(sulfone-amide) membranes. In this study, the removal of cast-solvent from the membrane was found to be a crucial factor to control the gas permeability, because the residual solvent affected the rearrangement of polymer chains in the membrane.

In chapter 7, a series of soluble poly(ether ketone) copolymers, in which *para*- and *meta*-phenylene contents are different, was prepared. Effects of polymer composition and thermal treatment of the poly(ether ketone) membranes on gas permeabilities of H₂, CO, O₂ and N₂ were studied. It was found that growth of crystalline region in the membranes with thermal treatment controlled the gas permeabilities.

REFERENCES

1. "Kouseinou Houkouzoku-kei Koubunshi Zairyou (High-performance Aromatic Polymer Materials)" (Ed. Society of Polymer Science, Japan), Maruzen, Tokyo(1990)
2. M.Kakimoto, M.Yoneyama, Y.Imai, *J. Polym. Sci., Polym. Chem. Ed.*, 26, 149(1988)
3. S.S.Mohite, N.N.Maldar and C.S.Marvel, *J. Polym. Sci., Polym. Chem. Ed.*, 26, 2777(1988)
4. Y.Oishi, S.Harada, M.Kakimoto and Y.Imai, *J. Polym. Sci., Polym. Chem. Ed.*, 27, 3393(1989)
5. A.E.Lozano, J.G.de la Campa and J.de Abajo, *Makromol. Chem., Rapid Commun.*, 11, 471(1990)
6. G.Liou, Y.Oishi, M.Kakimoto and Y.Imai, *J. Polym. Sci., Polym. Chem. Ed.*, 29, 995(1991)
7. J.Y.Jadhav, W.R.Krigbaum and J.Preston, *Macromolecules*, 21, 538(1988)
8. W.Hatke, H.Schmidt and W.Heitz, *J. Polym. Sci., Polym. Chem. Ed.*, 29, 1387(1991)
9. W.Hatke, H.Land, H.Schmidt and W.Heitz, *Makromol. Chem., Rapid Commun.*, 12, 235(1991)
10. R.J.Swedo and C.S.Marvel, *J. Polym. Sci., Polym. Lett. Ed.*, 15, 683(1977)
11. A.Sutter, P.Schmutz and C.S.Marvel, *J. Polym. Sci., Polym. Chem. Ed.*, 20, 609(1982)
12. J.Lee and C.S.Marvel, *J. Polym. Sci., Polym. Chem.*

Ed., 21, 2189(1983)

13. J.R.Havens and K.B.Reimer, *J. Polym. Sci., Polym.*

Chem. Ed., 27, 565(1989)

14. M.H.Yi, K.Choi and J.C.Jung, *J. Polym. Sci., Polym.*

Chem. Ed., 27, 2417(1989)

15. T.Takekoshi, *Advances in Polym. Sci.*, 94, 1(1990)

16. Y.Sakaguchi, *Kobunshi*, 41, 288(1992)

17. H.H.Yang, "Aromatic High-strength Fibers", P.66,

Wiley Interscience, New York(1989)

18. J.B.Rose, in "High Performance Polymers: Their Origin

and Development" P.187, Elsevier Science Publishing(1986)

19. M.J.Mullins and E.P.Woo, *J. Macromol. Sci., Rev.*

Macromol. Chem. Phys., C27, 313(1987)

20. M.I.Bessonov, M.M.Koton, V.V.Kudryavtsev and L.A.Laius,

"Polyimides — Thermally Stable Polymers", Plenum, New

York(1987)

21. V.T.Stannett, W.J.Koros, D.R.Paul, H.K.Lonsdale and

R.W.Baker, *Adv. Polym. Sci.*, 32, 69(1979)

22. J.H.Petropoulos, *Adv. Polym. Sci.*, 64, 93(1985)

23. K.Okamoto and H.Kita, *Hyomen*, 30, 210(1992)

24. T.Nakagawa, *Energy Shigen*, 6, 258(1985)

25. F.P.McCadless, *Ind. Eng. Chem. Process Des. Develop.*,

11, 470(1972)

Chapter-1

Synthesis and Characterization of Aromatic Polyamides

Derived from New Phenylated Aromatic Diamines

1-1 Introduction

Aromatic polyamides, such as poly(paraphenylene terephthalamide), show excellent mechanical properties and good thermal properties. However, these polymers are infusible and show limited solubility in organic solvents. There are general concepts for structural modification to improve the solubility of polymers as follows: introduction of flexible or kinked structure, decrease in structural regularity and symmetry, and incorporation of side chains or bulky substituents. To increase the solubility with maintaining the thermal stability of the polymers, the structural modification with whole aromatic system is particularly preferred.¹⁻¹⁰ From this view point, the introduction of phenyl side groups into the polymer chain is considered as an effective approach. In the case of aromatic rigid rod-like polyamides, several polymers having aromatic substituents have been reported to be soluble in organic solvents¹¹⁻¹⁴, and display anisotropic properties.¹¹⁻¹³ An advantage to obtain a soluble rigid rod-like polyamide lies in its possible application to the reinforcing material in molecular composite as well as the high-strength and high-modulus fiber.

In this chapter, the preparation of two new series of phenylated aromatic diamines and synthesis of poly-

mides derived from these diamines are described. Some characterizations of the polymers, such as thermal properties and solubility behavior are also reported.

1-2 Experimental

Materials

N-Methyl-2-pyrrolidone (NMP) was distilled over P_2O_5 under reduced pressure. Terephthaloyl chloride (TPC) and isophthaloyl chloride (IPC) were distilled under reduced pressure. Other chemicals were used without further purification.

Monomer Synthesis

1,4-Bis(1,3-dibenzoyl-2-propyl)benzene (3a)

Terephthalaldicarboxaldehyde (28.4g, 0.212mol) and acetophenone (152.1g, 1.27mol) were dissolved in 700ml of 95% ethanol. Potassium hydroxide (29.6g, 0.528mol) in 32ml of water was added to the solution dropwise. A precipitate appeared soon. The reaction mixture was stirred and refluxed for 3 hours, then filtered. The solid obtained was washed with 500ml of fresh 95% ethanol under reflux; Yield 11g (93%). mp 184-192°C (lit¹⁵. 204-205°C). ¹H-NMR ($CDCl_3$) δ =3.6 (d, 8H, CH_2), 4.2 (m, 2H,

CH), 7.4-7.8 (m, 16H, aromatic H), 8.2 (m, 8H, aromatic H).

1,4-Phenylenebis- γ,γ' -(2',6'-diphenylpyrylium)tetrafluoroborate (4a)

Triphenylmethanol (113.4g, 0.436mol) was dissolved in 700ml of acetic anhydride at 65°C, then the solution was cooled to room temperature with a water bath. 49% Fluoboric acid (78.0g, 0.435mol) was added dropwise maintaining the reaction at room temperature. Then, 3a (90.0g, 0.156mol) was added, and the resulting suspension was stirred for 17 hours. The product was collected, washed with THF several times, and then dried; Yield 106g (96%).

1,4-Bis(4-nitro-3,5-diphenylphenyl)benzene (5a)

Nitromethane (236g, 3.86mol) was added to a solution of potassium (15.5g, 0.396mol) in 580ml of *tert*-butanol. This solution was added to a stirred suspension of 4a (100g, 0.140mol) in 580ml of *tert*-butanol. Another solution of potassium (15.5g, 0.396mol) in 580ml of *tert*-butanol was added, then the mixture was stirred under reflux for 2 hours. The precipitate was collected, stirred in hot water, filtered, and dried; Yield 64.5g (74%). After the recrystallization from dioxane/ethanol

(4:1), the needles obtained showed the melting point at 341-344°C; IR(KBr) 1360 and 1530cm⁻¹ (NO₂). Anal. Calcd for C₄₂H₂₈N₂O₄: C, 80.75; H, 4.52; N, 4.48. Found: C, 80.37; H, 4.73; N, 4.36.

1,4-Bis(4-amino-3,5-diphenylphenyl)benzene (1a)

A suspension of 5a (12.0g, 0.0192mol) in 600ml of 2-methoxyethanol was stirred and heated to 100°C. Stannous chloride (48.7g, 0.216mol) which was dissolved in 115ml of hydrochloric acid was added to the suspension. After stirred around 100°C for 5 hours, the same amount of stannous chloride solution was added, and the reaction was continued for another 15 hours. The reaction mixture was poured into 1000ml of water and filtered. The solid obtained was neutralized by ammonium hydroxide, washed with water, and dried; Yield 10.6g (97%). The crude product was recrystallized from xylene several times; mp 310-312°C. IR (KBr) 3360 and 3450 cm⁻¹ (NH). Anal. Calcd for C₄₂H₃₂N₂: C, 89.33; H, 5.71; N, 4.96. Found: C, 89.52; H, 5.76; N, 4.71.

1,3-Bis(1,3-dibenzoyl-2-propyl)benzene (3b)

The reaction between isophthalaldicarboxaldehyde and acetophenone was carried out following a similar procedure to the preparation of 3a. During the reaction, two

phases were separated. The lower layer, which was viscous and dark brown, was separated and stirred with ethanol. After the ethanol was decanted, the viscous residue was dried; Yield 77%. ¹H-NMR (CDCl₃) δ=3.3 (d, 8H, CH₂), 4.0 (m, 2H, CH), 6.4-7.9 (m, 24H, aromatic H).

1,3-Phenylenebis-γ,γ'-(2,6-diphenylpyrylium)tetrafluoroborate (4b)

The procedure used in the preparation of 4a was applied to that of 4b; Yield 35%.

1,3-Bis(4-nitro-3,5-diphenylphenyl)benzene (5b)

A similar procedure to the preparation of 5a was applied to that of 5b. After the reaction, water was added to the reaction mixture. The precipitate was collected and dried; Yield 92%. mp 250-258°C. IR (KBr) 1360 and 1530 cm⁻¹ (NO₂).

1,3-Bis(4-amino-3,5-diphenylphenyl)benzene (1b)

The procedure used in the preparation of 1a was applied to that of 1b; Yield 97%. The crude product was recrystallized from toluene/ethanol. mp 212-213°C. IR (KBr) 3380 and 3480 cm⁻¹ (NH₂). Anal. Calcd for C₄₂H₃₂N₂: C, 89.33; H, 5.71; N, 4.96. Found: C, 89.78; H, 5.70; N, 4.71.

1,3-Bis(4-nitrophenyl)acetone (7)

4-Nitrophenylacetic acid (6) (100g, 0.552mol) was dissolved in 600ml of acetic anhydride. Keeping the system at 80°C, 300ml (2.16mol) of triethylamine was added dropwise and the solution was stirred for 2 hours. The solution was poured into 1000ml of 10% hydrochloric acid and filtered. The solid obtained was ground into a powder, and stirred in 500ml of refluxing concentrated hydrochloric acid for 8 hours. The product was collected and washed with water several times; Yield 79.8g (96%). IR (KBr) 1340 and 1520 cm^{-1} (NO_2), 1720 cm^{-1} (C=O). ^1H -NMR (CDCl_3) δ =8.0, 7.3 (dd, $J=8\text{Hz}$, aromatic H), 4.0 (s, 4H, CH_2).

2,5-Bis(4-nitrophenyl)-3,4-diphenylcyclopentadienone (8)

Benzil (54.6g, 0.260mol) and 7 (78.0g, 0.260mol) were added to 390ml of ethanol. After the stirred solution was heated nearly to the boiling point, a solution of 7.8g (0.139mol) of potassium hydroxide in 40ml of ethanol was added slowly. The reaction mixture was stirred for 1 hour, and then allowed to cool to room temperature. The product was collected and washed with ethanol several times; Yield 44g (36%). IR (KBr) 1340 and 1510 cm^{-1} (NO_2), 1715 cm^{-1} (C=O).

1,4-Bis(4-nitrophenyl)-2,3,5-triphenylbenzene (9a)

Phenylacetylene (19.3g, 0.189mol), 8 (30.0g, 0.063mol) and 130ml of *o*-dichlorobenzene was stirred at 180°C for two hours. The reaction mixture was allowed to cool to room temperature, and poured into 500ml of hexane. The product was collected by filtration and dried; Yield 22.9g (66%).

1,4-Bis(4-aminophenyl)-2,3,5-triphenylbenzene (2a)

A solution of 9a (20.0g, 0.0365mol) in 250ml of 2-methoxyethanol was stirred and heated to 80°C. A solution of stannous chloride (82.2g, 0.364mol) in 130ml of hydrochloric acid was added. Thereafter, the mixture was stirred around 100°C for 5 hours. The reaction mixture was allowed to cool to room temperature, and poured into 600ml of water and filtered. The solid obtained was neutralized by ammonium hydroxide, washed with water, and dried; Yield 10.0g (61%). The crude product was recrystallized from toluene; mp 256-258°C. IR (KBr) 3460 and 3480 cm^{-1} (NH_2). ^1H -NMR (CDCl_3) δ =3.3 (s, 4H, NH_2), 6.0-7.3 (m, 24H, aromatic H). Anal. Calcd for $\text{C}_{36}\text{H}_{28}\text{N}_2$: C, 88.49; H, 5.78; N, 5.73. Found: C, 88.85; H, 5.83; N, 5.58.

1,4-Bis(4-nitrophenyl)-2,3,5,6-tetraphenylbenzene (9b)

The procedure used in the preparation of 9a was applied to that of 9b, except the reaction time was extended to 17 hours; Yield 63%.

1,4-Bis(4-aminophenyl)-2,3,5,6-tetraphenylbenzene (2b)

The procedure used in the preparation of 2a was applied to that of 2b; Yield 45%. The crude product was recrystallized from pyridine; mp 453°C (DSC). IR (KBr) 3380 and 3450 cm^{-1} (NH_2). Anal. Calcd for $\text{C}_{42}\text{H}_{32}\text{N}_2$: C, 89.33; H, 5.71; N, 4.96. Found: C, 88.54; H, 5.64; N, 4.92.

Polymerization

As an example, the polymerization of 2a and terephthaloyl chloride (TPC) is shown below.

In a 25ml three-necked flask equipped with a mechanical stirrer, a nitrogen inlet, and a drying tube were placed 2a (0.4000g, 0.8187mol) and 2.9g of NMP. After the system was cooled below 5°C with an ice bath, TPC (0.1662g, 0.8186mol) was added and the reaction mixture was stirred for 30min. Thereafter, the reaction was continued at room temperature for 15 hours. The polymer solution was poured into 500ml of methanol. The polymer precipitated was collected and dried.

The other polymers were synthesized similarly. The polymerization concentrations were selected between 5% and 20%. When lithium carbonate or lithium chloride was added in the polymerization system, an equivalent with the amide linkages was added after the addition of the monomers.

Measurements

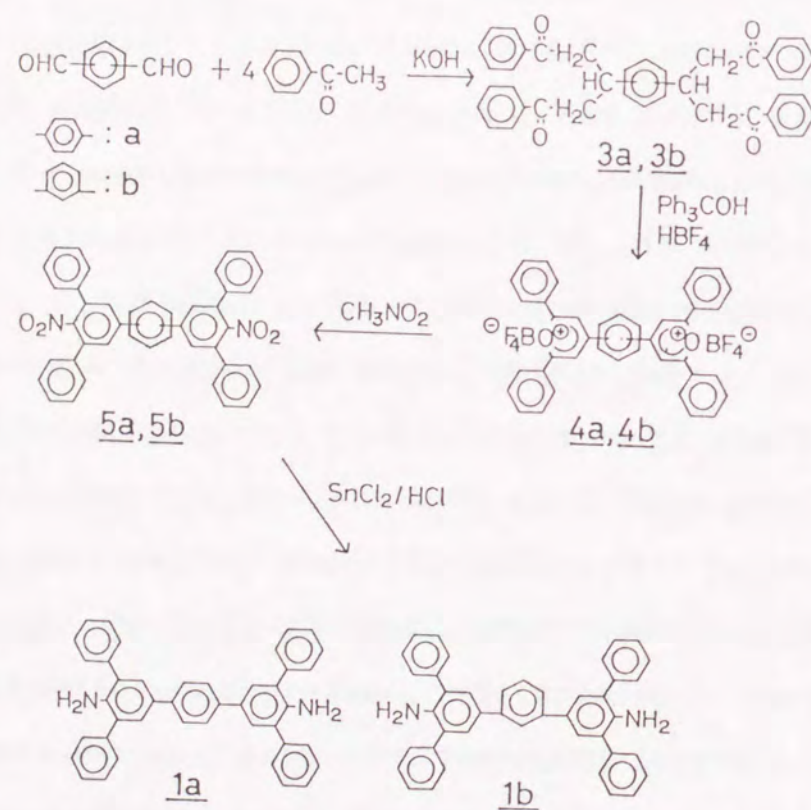
Inherent viscosities were measured at a concentration of 0.5g/dl in NMP with or without LiCl at 30°C. Infrared (IR) spectra were recorded on a Beckman FT2100 spectrometer with KBr disks. ^1H -NMR spectra were recorded on a Varian T60 NMR spectrometer. Thermogravimetric analysis (TGA) was conducted with a DuPont Model 951 thermogravimetric analyzer at a heating rate of 10°C/min in 100ml/min of N_2 or air flow. Differential scanning calorimetry (DSC) was performed on a DuPont 1090 thermal analyzer in combination with a DSC cell at a heating rate of 20°C/min in 60 ml/min of N_2 flow. Wide angle X-ray scattering (WAXS) was conducted on a Rigaku X-ray diffractometer with nickel-filtered $\text{CuK}\alpha$ radiation (38KV, 30mA) and a Laue camera. Solubility of the polymers was evaluated by mixing the polymers and solvents for 24 hours. Optical microscopic observation was carried out on a Nikon type 104 polarized-light transmission micro-

scope.

1-3 Results and Discussion

1-3-1 Monomer Synthesis

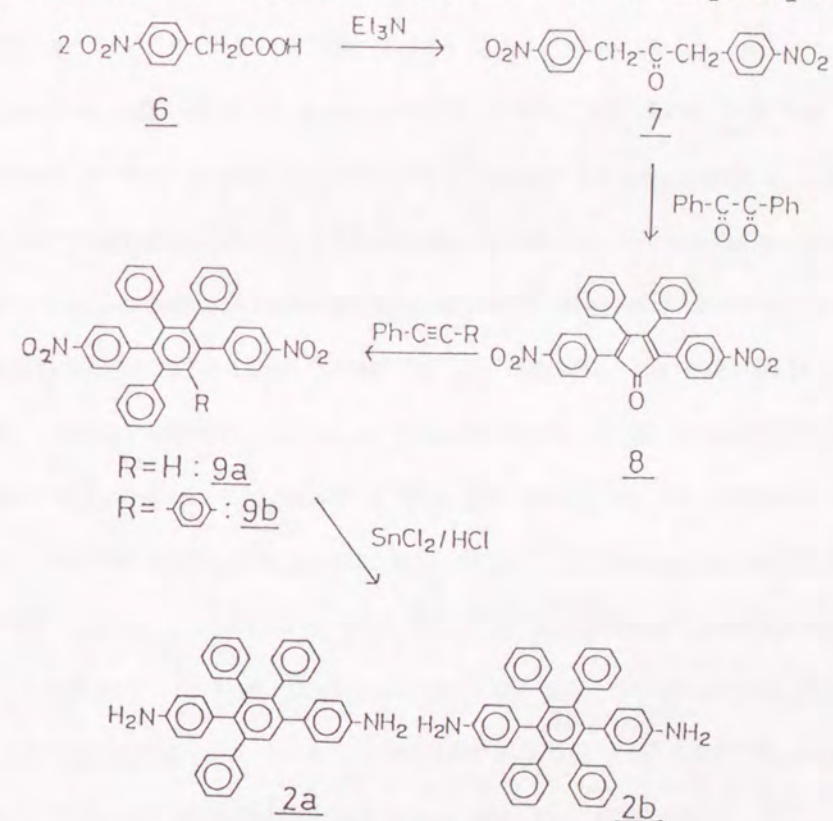
New diamines containing two phenyl groups on the *o*-positions with respect to the amino groups were prepared as shown in Scheme 1. Terephthalaldehyde and isophthalaldehyde were reacted with acetophenone to yield the tetraketones (3a¹⁵, 3b). The bispyrylium salts (4a, 4b) were derived from 3a and 3b, though rela-



Scheme 1

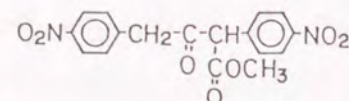
tively long reaction time (17 hours) was necessary due to the heterogeneous reaction. The dinitro compounds (5a, 5b) were prepared by using a method for the condensation of 2,4,6-triphenylpyrylium tetrafluoroborate and nitromethane in the presence of potassium *tert*-butoxide.¹⁶ The diamines (1a, 1b) were obtained by the reduction of 5a and 5b with stannous chloride as a reducing agent. In the case of 1a, the yield was sometimes low because the solubility of 5a was poor.

The other new diamines containing phenyl groups on the middle phenylene of *p*-terphenylene were prepared as shown in Scheme 2. Condensation of 4-nitrophenylacetic



Scheme 2

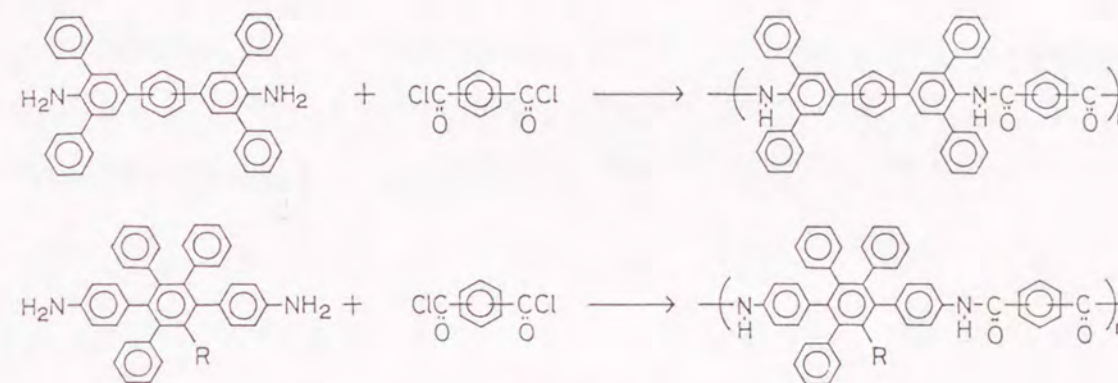
acid was carried out following a literature¹⁷. The product obtained had a structure as shown below, and the



decarboxylation under reflux of concentrated hydrochloric acid gave 1,3-bis(4-nitrophenyl)acetone (7). The cyclopentadienone (8) was synthesized by using a similar method to the preparation of tetraphenylpentadienone.¹⁸ The dinitro compounds (9a, 9b) were prepared by the Diels-Alder reaction.¹⁹ Because of steric hindrance, the reaction of 8 and diphenylacetylene needed a longer reaction time (17 hours) than that of 8 and phenylacetylene. The diamines (2a, 2b) were obtained by the reduction of 9a and 9b with stannous chloride as a reducing agent. Recrystallization of 2b was carried out from pyridine due to poor solubility in xylene or toluene, which was used for the recrystallization of the other three diamines. Pure 2b showed a sharp endothermic peak at 453°C on a DSC measurement. It seems that the highly symmetrical structure of 2b made the thermal stability of crystal extremely high in comparison with the other diamines prepared.

1-3-2 Polymerization

Polymerization of the diamines and terephthaloyl chloride (TPC) or isophthaloyl chloride (IPC) was carried out by low-temperature solution condensation in NMP (Scheme 3). The results are summarized in Table I.



Scheme 3

Precipitate of 1a/TPC polyamide appeared during the polymerization in NMP. When polymerized in the presence of Li₂CO₃, the reaction mixture was a clear solution and gave the polymer with inherent viscosity of 0.97 dl/g. However, the molecular weight was not high enough to form a film. Polymers, 1a/IPC, 1b/TPC and 1b/IPC were polymerized as homogeneous solutions. The polymers 1a/IPC and 1b/TPC gave flexible and tough films. Relatively low viscosities of these polymers may be attributed to the steric hindrance of the diamines due to the bulky side groups on the *o*-position of the amino groups.

Table I. Synthesis of Polyamides

Diamine	Diacid Chloride	Condition		Outlook	Yield (%)	$\eta_{inh}^{1)}$ (dl/g)	film
		Conc.	Additive				
<u>1a</u>	TPC	5%	no	turbid	89	0.83	no
	TPC	7%	Li ₂ CO ₃	transparent	85	0.97	no
	IPC	7%	no	"	93	0.47	yes
<u>1b</u>	TPC	8%	no	"	99	0.62	yes
	IPC	13%	no	"	89	0.28	no
<u>2a</u>	TPC	14%	no	"	97	2.87	yes
	IPC	14%	no	"	97	0.88	yes
<u>2b</u>	TPC	8%	no	precipitate	78	0.46 ²⁾	no
	TPC	14%	LiCl	cloudy	83	0.93 ²⁾	no
	IPC	14%	no	precipitate	91	0.49 ²⁾	yes
	IPC	15%	LiCl	cloudy	81	0.46 ²⁾	yes

1) Inherent viscosity measured at a concentration of 0.5g/dl in NMP at 30°C except for 2).

2) NMP containing LiCl was used as a solvent.

The polymerization using 2a gave polyamides having good solubility and high viscosity to form tough films. The polymer made of 2a and TPC gave the highest inherent viscosity of 2.87 dl/g in this series. In the case of 2b, on the other hand, both polymers derived from TPC and IPC precipitated during the polymerization in NMP. The polymerization in the presence of LiCl did not improve the solubility remarkably, and did not increase the inherent viscosity so much.

1-3-3 Characterization

Thermal transition behavior was evaluated by DSC measurements. The polymers containing *m*-catenation showed the glass transitions at 275-349°C, except for 2b/IPC polyamide (Table II). The polymers in which all linkages are *p*-catenated did not show clear glass transition. All the polymers did not show melting behavior below their decomposition temperatures, though X-ray diffraction measurements showed that the polymers had more or less semi-crystalline characteristics. The X-ray diffraction photograph of 2a/TPC is shown in Figure 1 as an example.

All the polymers showed good thermal stability on the TGA measurements; 5% weight-loss temperatures were in the range of 466-524°C. There was no remarkable difference in measuring atmosphere, N₂ or air.

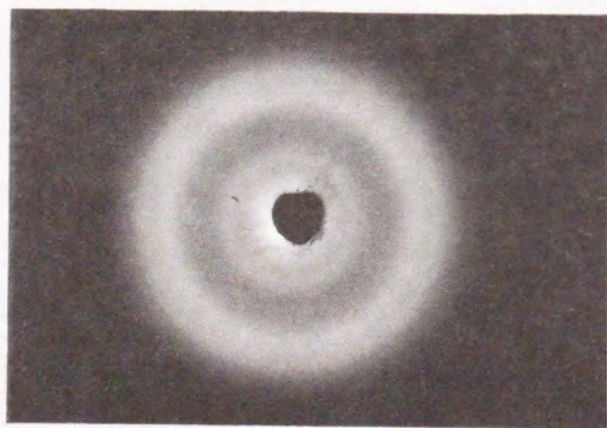


Figure 1. X-ray diffraction photograph of the 2a/TPC polyamide

Table II. Characterization of Polyamides

Polymer		η_{inh} (dl/g)	$T_g^{1)}$ (°C)	TGA ²⁾ (°C)		Solubility ³⁾	
Diamine	Diacid Chloride			N ₂	air	NMP	CHCl ₃
<u>1a</u>	TPC	0.97	—	508	482	+	-
	IPC	0.47	299	482	485	++	-
<u>1b</u>	TPC	0.62	327	477	467	++	-
	IPC	0.28	275	466	467	++	-
<u>2a</u>	TPC	2.87	—	508	493	++	-
	IPC	0.88	349	509	520	++	-
<u>2b</u>	TPC	0.93	—	516	524	-	-
	IPC	0.49	—	514	516	-	-

- 1) T_g determined by DSC at a heating rate of 20°C/min in N₂.
 2) 5% weight-loss temperature on TGA at a heating rate of 10°C/min in 100ml/min flow of N₂ or air.
 3) ++: soluble, +: partially soluble, -: insoluble.

The polymers derived from 1b and 2a showed good solubility in NMP. The flexible structure by m-catenation in the former and the interference of polymer chain packing by the unsymmetrical structure in the latter contributed to improve their solubilities. The diamines which have p-catenated and symmetrical structure (1a and 2b) made the polymers less soluble in NMP. Monomer crystallinity of 2b, which showed an extremely high melting temperature, may be responsible for the lowest solubility of the polymers derived from 2b in this series.

In the three rigid rod-like polyamides, 2a/TPC polyamide showed the highest viscosity and the best solubility. Preliminary microscopic observation of 2a/TPC polyamide solution in NMP was carried out at room temperature. A 20% solution was obtained from the polymerization solution directly, and observed through an optical microscope under crossed polarization. Some part of the solution showed colorful birefringence and the other part showed monochromic birefringence. In the case of a 20% NMP solution containing LiCl, some part showed colorful birefringence, and the other part showed color only under applied shear, and relaxed to an isotropic phase quickly. The relation of microscopic appearance and polymer concentration is listed in Table III. These

anisotropic behaviors suggest that 2a/TPC polyamide solution in NMP forms a liquid crystalline phase.

Table III. Microscopic observation of 2a/TPC polyamide solution in NMP containing LiCl under crossed polarization.

Polymer Concentration	Under Shear	No Shear
20%	colorful birefringence	partially colorful birefringence
17%	colorful birefringence	monochromic birefringence
15%	bright \longleftrightarrow dark	dark
10%	slightly bright \leftrightarrow dark	dark
5%	dark	dark

1-4 Conclusions

Four new phenylated aromatic diamines, 1,4-bis(4-amino-3,5-diphenylphenyl)benzene (1a), 1,3-bis(4-amino-3,5-diphenylphenyl)benzene (1b), 1,4-bis(4-aminophenyl)-2,3,5-triphenylbenzene (2a) and 1,4-bis(4-aminophenyl)-2,3,5,6-tetraphenylbenzene (2b) were synthesized and polymerized with terephthaloyl chloride (TPC) and isophthaloyl chloride (IPC). All the polyamides showed high thermal stability with 5% weight-loss temperatures in the range of 466-524°C in air or nitrogen, and no melting peak below their decomposition temperatures. The polymers containing *m*-catenation had glass transition temperatures in the range of 275-349°C, and were soluble in *N*-methyl-2-pyrrolidone (NMP). The rigid rod-like polyamides consisting of all para-oriented linkages showed no clear glass transition. In the rod-like polymers, polymer 2a/TPC showed good solubility in NMP, and preliminary optical microscope observation for the 20% solution showed an anisotropic property.

REFERENCES

1. M.Kakimoto, M.Yoneyama and Y.Imai, *J. Polym. Sci., Polym. Chem. Ed.*, 26, 149(1988)
2. S.S.Mohite, N.N.Maldar and C.S.Marvel, *J. Polym. Sci., Polym. Chem. Ed.*, 26, 2777(1988)
3. F.Akutsu, K.Matsuo, K.Naruchi and M.Miura, *Polym. Commun.*, 30, 182(1989)
4. Y.Oishi, S.Harada, M.Kakimoto and Y.Imai, *J. Polym. Sci., Polym. Chem. Ed.*, 27, 3393(1989)
5. A.E.Lozano, J.G.de la Campa and J.de Abajo, *Makromol. Chem., Rapid Commun.*, 11, 471(1990)
6. Y.Oishi, H.Takado, M.Yoneyama, M.Kakimoto and Y.Imai, *J. Polym. Sci., Polym. Chem. Ed.*, 28, 1763(1990)
7. J.Lin, Y.Yuki, H.Kunisada and S.Kondo, *J. Appl. Polym. Sci.*, 40, 2113(1990)
8. M.Xie, Y.Oishi, M.Kakimoto and Y.Imai, *J. Polym. Sci., Polym. Chem. Ed.*, 29, 55(1991)
9. H.Jeong, M.Kakimoto and Y.Imai, *J. Polym. Sci., Polym. Chem. Ed.*, 29, 767(1991)
10. G.Liou, Y.Oishi, M.Kakimoto and Y.Imai, *J. Polym. Sci., Polym. Chem. Ed.*, 29, 995(1991)
11. J.Y.Jadhav, W.R.Krigbaum and J.Preston, *Macromolecules*, 21, 538(1988)
12. J.Y.Jadhav and W.R.Krigbaum, *J. Polym. Sci., Polym. Chem. Ed.*, 27, 1175(1989)

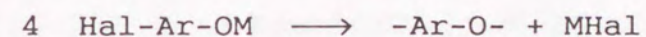
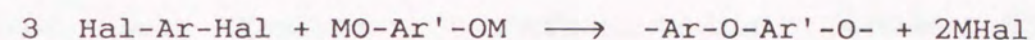
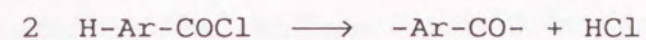
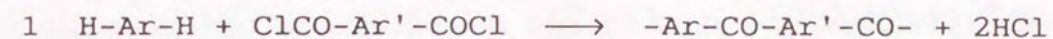
13. W.Hatke, H.Schmidt and W.Heitz, *J. Polym. Sci., Polym. Chem. Ed.*, 29, 1387(1991)
14. W.Hatke, H.Land, H.Schmidt and W.Heitz, *Makromol. Chem., Rapid Commun.*, 12, 235(1991)
15. S.V.Krivun and G.N.Dorofeenko, *Khim. Getero. Soedi.*, 2, 656(1966)
16. W.Foerst, "Newer Method of Preparative Organic Chemistry", Vol.III, 415, Academic Press (1964)
17. H.Saikachi and Y.Taniguchi, *Yakugaku Zasshi*, 88, 1054 (1968)
18. E.C.Horning, Ed."Org. Syn." Coll. Vol. 3, John Wiley & Sons, New York, P.806(1955)
19. L.F.Fieser, "Organic Experiments", 2nd Ed., Heath, D.C. Co., Lexington, MA, P.297(1968)

Chapter-2

Synthesis of Poly(ether ketone) by Friedel-Crafts
Acylation: Effects of Reaction Conditions

2-1 Introduction

Poly(arylene ether ketone)s (PEK) are well-known high performance semi-crystalline polymers having high thermal stability and excellent mechanical property. Synthesis of PEKs is classified into two methods^{1,2}: (1) acylation method in which ketone linkages are formed (equations 1 and 2), (2) aromatic nucleophilic displacement method between activated aromatic halides and alkali metal phenoxides in which ether linkages are formed (equations 3 and 4).



In the acylation method, Friedel-Crafts acylations are carried out either in an organic solvent with aluminum trichloride as a catalyst^{3,4} or in hydrogen fluoride / boron trifluoride system as a catalyst and solvent.^{5,6} Alternatively, the polymerization involves dehydrative acylation reactions in polyphosphoric acid,^{7,8} in trifluoromethanesulfonic acid,⁹ and in methanesulfonic acid / phosphorus pentoxide medium.¹⁰

The polycondensation in an organic solvent catalyzed by aluminum trichloride can be carried out under moderate conditions, and considered as a convenient method to

obtain PEKs in laboratory scale. An AA-BB type polymerization such as a reaction between diphenyl ether and isophthaloyl chloride and an AB type polymerization such as a self-condensation of 4-phenoxybenzoyl chloride are possible. Therefore, various combinations of monomers afford a number of structures of polymers.¹¹⁻¹⁷

However, reaction behavior of the Friedel-Crafts polyacylation has not been reported in detail. Especially, in the polymerization in 1,2-dichloroethane with aluminum trichloride catalyst, polymer/catalyst complexes⁶ precipitate during the reaction, which thereby displays a different outlook from general solution polycondensations. In this chapter, the synthesis of poly(ether ketone) by Friedel-Crafts acylation was examined using the reaction between diphenyl ether and isophthaloyl chloride.

2-2 Experimental

Materials

Isophthaloyl chloride (IPC, Mitsubishi Gas chemical Co., Inc.) and aluminum trichloride (AlCl_3 , Nacalai Tesque, EP) were ground to powders in nitrogen atmosphere. 1,2-Dichloroethane (DCE, Nacalai Tesque, GR) was dried over molecular sieves. Diphenyl ether (DPE, Nacalai Tesque, GR) was used without further purification.

Polymerization

A standard procedure for the preparation of poly(ether ketone) is described below. In a 300ml four-necked flask equipped with a nitrogen inlet and a stirring rod, 12.22g of DPE (0.07182mol) and 14.58g of IPC (0.07182mol) were dissolved in 200ml of DCE. After the solution was cooled below 5°C with an ice bath, 24.96g of AlCl_3 (0.1872mol) was added, and the reaction mixture was stirred for 2 hours. Thereafter, the reaction was continued at room temperature for 16 hours. The DCE was decanted from the reaction mixture, the obtained mass was mixed with methanol to decompose the complex, and the methanol supernatant was removed by filtration. The product was washed with 10% hydrochloric acid twice, and then with water several times by using a blender. The polymer was dried at 150°C under vacuum for 17 hours.

The reaction behavior was examined under different reaction conditions.

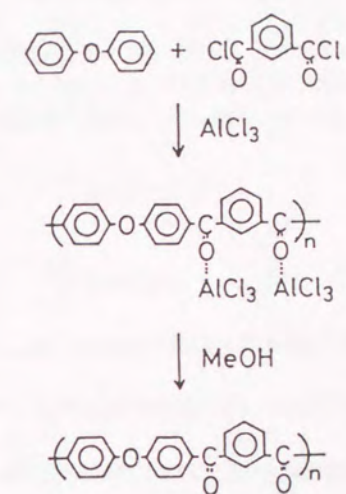
Characterization

Inherent viscosities were measured with an Ostwald type viscometer at 0.1g/dl in 95% sulfuric acid at 30°C. Infrared spectra were recorded on a Hitachi 270-30 Infrared spectrometer with KBr disks. NMR spectra were measured on a Varian Gemini-200 spectrometer in a mixture of dichloromethane- d_2 and trifluoroacetic acid- d .

2-3 Results and Discussion

2-3-1 Influence of Reaction Conditions on PEK Polymerization

The preparation of poly(ether ketone) (PEK) from diphenyl ether (DPE) and isophthaloyl chloride (IPC) by Friedel-Crafts acylation with aluminum trichloride ($AlCl_3$) was studied (Scheme 1).



Scheme 1

Figure 1 shows a change in the inherent viscosity of the polymers with reaction time at a polymer concentration of 8wt% in 1,2-dichloroethane (DCE). The polymerization was carried out below 5°C for first 2 hours, then at room temperature. The molar ratio of $AlCl_3$ to IPC was 2.6. When the reaction proceeded for 1 - 2 hours, a precipitation occurred, and thereafter the amount of

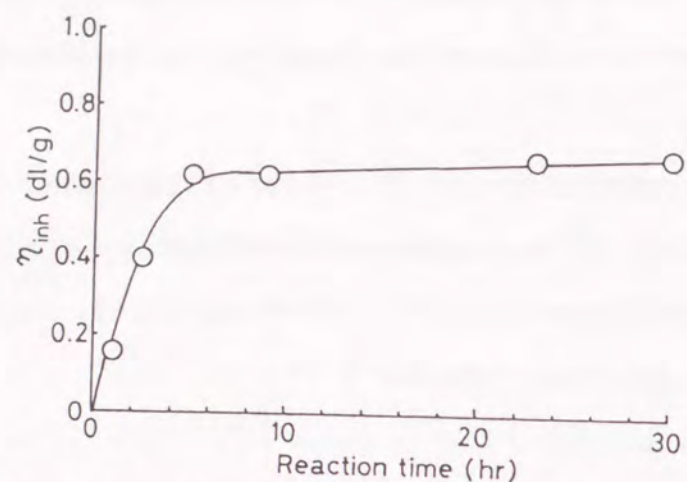


Figure 1. change in the inherent viscosity of poly(ether ketone) with reaction time with a polymer concentration of 8wt% at room temperature. Viscometry in 95% sulfuric acid at 30°C.

precipitate increased gradually. The inherent viscosity almost leveled off within 5 hours.

In general, Friedel-Crafts acylation gives a 1:1 complex of $AlCl_3$ and the carbonyl group formed.¹⁸⁻²⁰ Therefore, an excess of $AlCl_3$ more than molar equivalent with the carbonyl groups formed should be used to catalyze the reaction. In the preparation of PEK, formation of the same type of complexes has been also reported,⁶ and a similar effect in the feed ratio of $AlCl_3$ and IPC was obtained as shown in Table I; the reaction with $AlCl_3$ two equivalents to IPC gave the polymer which had a low inherent viscosity of 0.27 dl/g, and an excess of $AlCl_3$

Table I. Effect of $AlCl_3$ quantity on PEK polymerization

$AlCl_3$ (molar ratio to IPC)	Yield (%)	$\eta_{inh}^{2)}$ (dl/g)
2.0	89	0.27
2.6	95	0.68
3.0	95	0.74
4.0	90	0.68

1) Polymerized at room temperature with a polymer concentration of 8wt% for 16 hours.

2) Measured with a concentration of 0.1 g/dl in 95% sulfuric acid at 30°C.

over the monomer is necessary to obtain the polymers with higher viscosities. However, large excess of $AlCl_3$ such as a 4-fold excess seems to induce unfavored side reactions, since the polymer obtained under this condition contained a fraction insoluble in 95% sulfuric acid. Therefore, the suitable quantity of $AlCl_3$ was 2 to 3 equivalents to IPC.

The effect of reaction temperature is shown in Table II. Although the reaction at room temperature gave polymers completely soluble in sulfuric acid, higher reaction temperatures resulted in an insoluble part. When polymerized at 85°C, the polymer obtained was completely insoluble in sulfuric acid, and the yield (109%)

Table II. Effect of reaction temperature on PEK Polymerization

Temperature (°C)	Yield (%)	$\eta_{inh}^{2)}$ (dl/g)	Solubility in H ₂ SO ₄
r.t.	95	0.68	soluble
50	94	0.66	some insoluble part
85	109	—	insoluble

1) Polymerized at a polymer concentration of 8wt% with 2.6 molar ratio of AlCl₃ for 16 hours.

2) Measured with a concentration of 0.1 g/dl in 95% sulfuric acid at 30°C.

was higher than the theoretical value. Figure 2 compares the IR spectra of the polymers obtained at room temperature and at 85°C. The polymer obtained at 85°C showed the sp³ C-H stretching at 2900-3000 cm⁻¹. This means that the Friedel-Crafts alkylation with DCE occurred as a side reaction, and a cross-linked polymer was obtained.

Table III shows the effect of the DPE/IPC feed ratio on the inherent viscosity of the polymer obtained. A monomer ratio of 1:1 gave the maximum inherent viscosity, and deviations from the stoichiometry gave lower viscosities. Although this polymerization involved the precipitation of polymer/AlCl₃ complexes during the reaction, the molar ratio effect was similar to those in the usual solution polycondensation reactions.

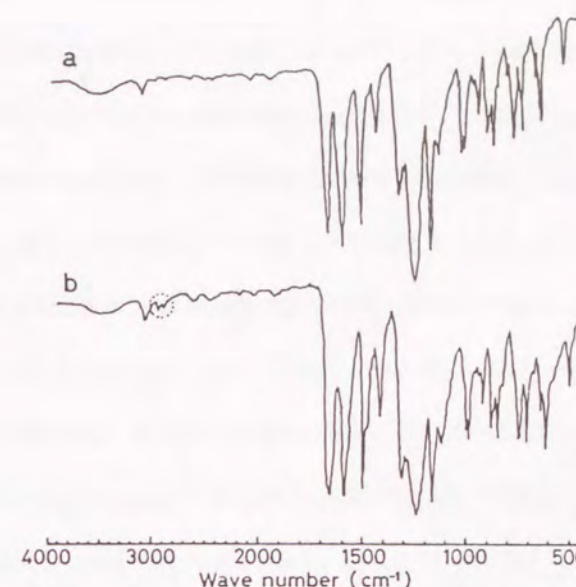


Figure 2. IR spectra of poly(ether ketone) polymerized at: (a) room temperature; (b) 85°C.

Table III. Effect of monomer ratio on PEK polymerization

Monomer ratio		Yield (%)	$\eta_{inh}^{2)}$ (dl/g)
DPE	IPC		
1.00	0.99	90	0.57
1.00	1.00	95	0.68
1.00	1.01	92	0.47

1) Polymerized at room temperature at a polymer concentration of 8wt% with 2.6 molar ratio of AlCl₃ for 16 hours.

2) Measured with a concentration of 0.1 g/dl in 95% sulfuric acid at 30°C.

The acylation-type polymerization also showed a characteristic effect of the monomer concentration on the inherent viscosity of the polymers. As shown in Table IV, lower monomer concentrations resulted in higher viscosities. At 8wt% of the monomers, the reaction formed a gelatinous mass and gave an inherent viscosity of 0.68 dl/g. On the other hand, at 2.5wt% the polymerization gave a number of hexagonal grains of several millimeters that were apparently single crystals, and the inherent viscosity was 0.87 dl/g. Therefore, such a difference in the feature of precipitates seems to affect the polymerization. This effect will be discussed in the next section.

Table IV. Effect of polymer concentration on PEK polymerization

Polymer Concentration (wt%)	Yield (%)	$\eta_{inh}^{2)}$ (dl/g)
19	95	0.57
8	95	0.68
4	94	0.75
2.5	97	0.87

1) Polymerized at room temperature with 2.6 molar ratio of $AlCl_3$ for 16 hours.

2) Measured with a concentration of 0.1 g/dl in 95% sulfuric acid at 30°C.

2-3-2 Polymerization Behavior in the Polymer Precipitate

An effect of the formation of precipitates on the polymerization rate was examined. The polymerization was terminated at several reaction periods described in Table V. After separating the precipitate and the solution, both parts were treated with methanol to obtain the products. As shown in Table V, the substances remaining in the solution was a PEK oligomer having an inherent viscosity around 0.1 dl/g, and when the viscosity exceeded 0.2 dl/g the precipitation occurred. Thereafter, the quantity of precipitate and the inherent viscosity increased with reaction time. Because the increase in

Table V. Polymerization behavior of PEK

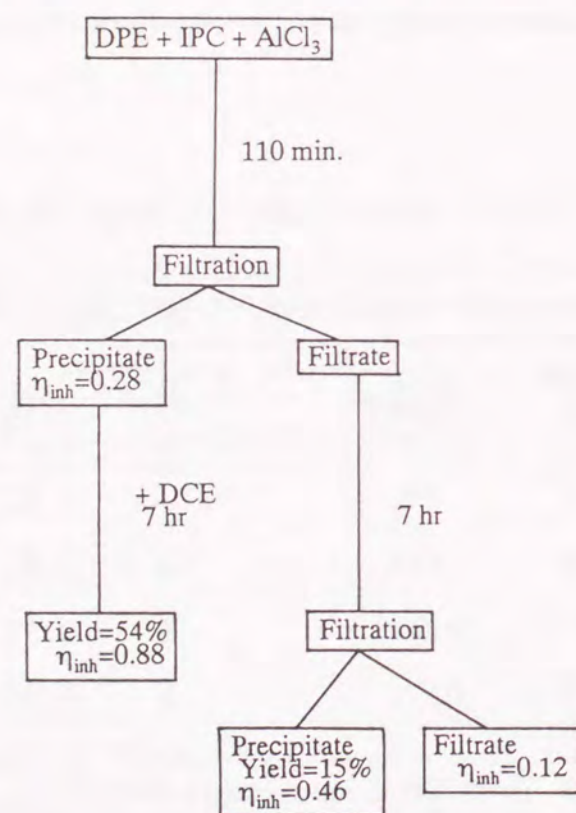
Reaction time (hr)	from gelatinous mass		from solution		Total Yield (%)
	Yield (%)	$\eta_{inh}^{2)}$ (dl/g)	Yield (%)	$\eta_{inh}^{2)}$ (dl/g)	
1	0	—	—	0.13	—
1.5	65	0.24	20	0.12	85
2.5	81	0.44	5	0.14	86
5.0	91	0.71	1	0.10	93

1) Polymerized at room temperature at a polymer concentration of 8wt% with 2.6 molar ratio of $AlCl_3$.

2) Measured with a concentration of 0.1 g/dl in 95% sulfuric acid at 30°C.

the viscosity was remarkable compared to that of the precipitate quantity, it seems that the reaction could proceed in solid state.

To clarify the possibility of the reaction between the TPC chain-end and DPE chain-end in the precipitate, in addition to the reaction between a chain-end in the precipitate and a monomer or oligomer in the solution, an experiment described in Scheme 2 was carried out. The precipitate that appeared at early stage was separated, to which fresh DCE was added. Without any additional supply of the monomers or oligomers, the polymerization



Scheme 2

proceeded in the precipitate, where the inherent viscosity increased from 0.28 to 0.88 dl/g in 7 hours. From this result, the reaction between the two chain-ends in the precipitate was confirmed.

The crystalline-like precipitate formed during the polymerization at a lower concentration seems to have an advantage in the reaction between the chain-ends due to the regular alignment of the polymer chains. This is considered to be a reason why polymerization at a lower concentration gave a higher inherent viscosity.

Fresh DCE added to the precipitate may extract hydrogen chloride formed by the acylation reaction to induce the polymerization. On the basis of this idea, solvent exchange, namely, the polymerization, in which the DCE was removed from the precipitate and fresh DCE was added several times, was attempted. Table VI and VII show the results of the solvent exchange experiments at polymer concentrations of 8wt% and 19wt%, respectively. The polymerization without the solvent exchange resulted in polymers having the inherent viscosities of 0.68 and 0.57 dl/g, respectively (Table IV, the first two lines). The solvent exchange method, in contrast, gave higher molecular weight polymers ($\eta_{inh} = 0.92$ and 0.68 dl/g, at 8 and 19wt%, respectively).

Table VI. PEK polymerization with solvent exchange at 8wt%

Reaction time (hr)	$\eta_{inh}^{1)}$ (dl/g)	solvent exchange ²⁾
2.5	—	done
5.0	0.78	done
23.0	0.92	—

1) Measured with a concentration of 0.1 g/dl in 95% sulfuric acid at 30°C.

2) Solvent exchange: extraction of 100ml of DCE from the reaction mixture and then addition of 100ml of fresh DCE.

Table VII. PEK polymerization with solvent exchange at 19wt%

Reaction time (hr)	$\eta_{inh}^{1)}$ (dl/g)	solvent exchange ²⁾
2.0	0.34	done
2.5	0.46	done
3.5	0.48	done
5.5	0.58	done
21.0	0.68	—

1) Measured with a concentration of 0.1 g/dl in 95% sulfuric acid at 30°C.

2) Solvent exchange: extraction of 100ml of DCE from the reaction mixture and then addition of 100ml of fresh DCE.

Figure 3 shows the advantage of the solvent exchange for a wide range of polymer concentrations. Especially at lower concentrations, the effect of the solvent exchange was remarkable. This effect is attributed to the formation of the crystalline-like precipitate at lower concentrations, which accelerates the reaction between the polymer chain-ends.

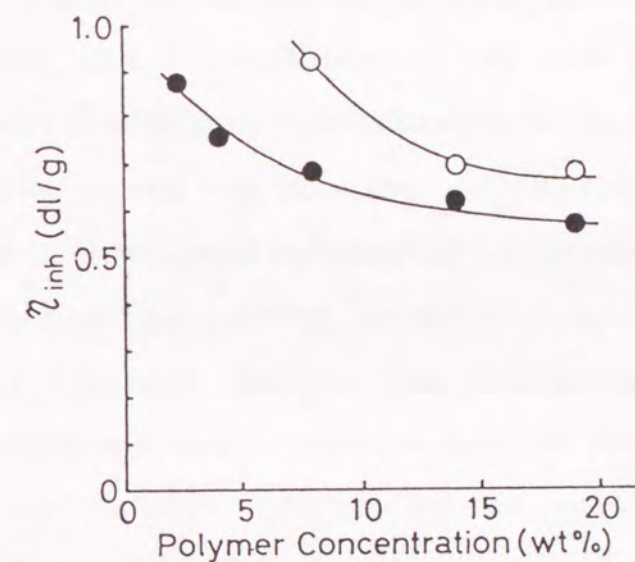


Figure 3. Effect of the solvent exchange operation on the inherent viscosity of polymers: O, with the solvent exchange; ●, without the solvent exchange.

2-4 Conclusions

The influence of reaction conditions on the Friedel-Crafts polycondensation of diphenyl ether and isophthaloyl chloride in 1,2-dichloroethane with aluminum trichloride catalyst was examined. The 1:1 DPE/IPC monomer ratio, AlCl_3 with a 2 - 3-fold molar excess over IPC, and a lower reaction temperature gave PEK with a sufficiently high molecular weight and a good solubility in 95% sulfuric acid. The polymerization formed a precipitate of polymer/catalyst complexes, and it proceeded even in the precipitate through the reaction between the polymer chain-ends. When the polymerization was performed at a low polymer concentration, crystalline-like grains appeared and the reaction between the chain-ends was accelerated. Contacting the precipitate with fresh solvent, i.e., the solvent exchange procedure, was effective to induce a further polymerization, because the hydrogen chloride formed by the acylation was easily removed from the reaction site.

REFERENCES

1. J.B.Rose, "High Performance Polymers: Their Origin and Development" (Ed. R.B.Seymour and G.S.Kirshenbaum), Elsevier Science Publishing, pp.187-193(1986)
2. M.J.Mullins and E.P.Woo, *J. Macromol. Sci., Rev. Macromol. Chem. Phys.*, C27, 313(1987)
3. W.H.Bonner, U.S.Patent 3,065,205(1962)
4. I.Goodman, J.E.McIntyre and W.Russell, British Patent 971,227(1964)
5. B.M.Marks, U.S.Patent 3,442,857(1969)
6. V.Jansons and K.Dahl, *Makromol. Chem., Macromol. Symp.*, 51, 87(1991)
7. Y.Iwakura, K.Uno and T.Takiguchi, *J. Polym. Sci., A-1*, 6, 3345(1968)
8. Y.Iwakura, K.Uno and T.Takiguchi, *J. Polym. Sci., Polym. Lett. Ed.*, 15, 283(1977)
9. W.Risse, D.Y.Sogah and F.P.Boettcher, *Makromol. Chem., Macromol. Symp.*, 44, 185(1991)
10. M.Ueda and M.Sato, *Macromolecules*, 20, 2675(1987)
11. R.J.Swedo and C.S.Marvel, *J. Polym. Sci., Polym. Lett. Ed.*, 15, 683(1977)
12. A.Sutter, P.Schmutz and C.S.Marvel, *J. Polym. Sci., Polym. Chem. Ed.*, 20, 609(1982)
13. J.Lee and C.S.Marvel, *J. Polym. Sci., Polym. Chem. Ed.*, 21, 2189(1983)

14. T.Ogawa and C.S.Marvel, *J. Appl. Polym. Sci.*, 33, 1579(1987)
15. T.Ogawa and C.S.Marvel, *J. Polym. Sci., Polym. Chem. Ed.*, 25, 251(1987)
16. J.R.Havens and K.B.Reimer, *J. Polym. Sci., Polym. Chem. Ed.*, 27, 565(1989)
17. M.H.Yi, K.Choi and J.C.Jung, *J. Polym. Sci., Polym. Chem. Ed.*, 27, 2417(1989)
18. N.O.Calloway, *Chem. Rev.*, 17, 327(1935)
19. G.A.Olah, Ed. "*Friedel-Crafts and Related Reactions*", Interscience, New York, Vol.1, P.569(1963); Vol.3, P.1003 (1964)
20. L.K.Tan and S.J.Brownstein, *J. Org. Chem.*, 47, 4737 (1982)

Chapter-3

Synthesis of Polyimide and Poly(imide-benzoxazole) in Polyphosphoric Acid

3-1 Introduction

Polyimides are well-known as excellent heat- and chemical-resistant polymers.^{1,2} Because of their poor tractability, the soluble precursor, polyamic acids, are synthesized in an organic solvent such as *N*-methyl-2-pyrrolidone (NMP), and cast to a film or spun to a fiber, then imidized thermally or chemically. To improve their tractability, modifications of the polymer structures have been made by introducing bulky substituents, flexible linkages, etc.^{1,3} These soluble polyimides can be prepared by the polymerization followed by chemical or thermal imidization in a one-pot solution.

In this study, polyphosphoric acid was employed as a solvent to prepare polyimides. polyphosphoric acid has good properties for solubilization and dehydration of many organic compounds. Therefore, it is used to synthesize the heterocycles-containing polymers^{4,5} such as polybenzimidazoles (PBI)⁶, polybenzothiazoles (PBT)⁷⁻¹⁰ and polybenzoxazoles (PBO)^{8,9,11}, and other polymers like poly(ether ketone)s¹². There is only one report about the synthesis of polyimides in polyphosphoric acid, in which polyimides derived from 2,3,5,6-pyridinetetracarboxylic acid and various aromatic diamines were prepared.¹³ However, these polymers showed poor properties and the details of the reaction was not discussed.

In this chapter, the possibility of polyphosphoric acid for a polymerization medium of polyimides was examined in detail, and a polyimide which had a high enough molecular weight to form a film was prepared for the first time in polyphosphoric acid.

This imide-formation reaction in polyphosphoric acid could also be applied to the one-pot preparation of a copolymer containing imide and heterocyclic rings alternately.

3-2 Experimental

Materials

3,3'-Dihydroxy-4,4'-diaminobiphenyl (HAB, Wakayama Seika Kogyo Co., Ltd.) was purified as a hydrochloride by the recrystallization from dilute aqueous hydrochloric acid. 4,4'-Diaminodiphenyl ether (ODA, Nacalai Tesque, GR), 3,3',4,4'-biphenyltetracarboxylic dianhydride (BPDA, Ube Industries, Ltd.), 4-aminobenzoic acid (ABA, Nacalai Tesque, GR), 75.5% polyphosphoric acid (PPA, Nacalai Tesque), phosphorus pentoxide (P_2O_5 , Nacalai Tesque, GR), aniline (Nacalai Tesque, GR) and phthalic anhydride (Nacalai Tesque, GR) were used without further purification. *o*-Chlorophenol (Nacalai Tesque, EP) and *m*-cresol

(Nacalai Tesque, GR) were purified by distillation. *N*-Methyl-2-pyrrolidone (NMP, Mitsubishi Kasei Corp.) was dried over molecular sieves for more than one day before use.

Model reaction in PPA

Phosphorus pentoxide (P_2O_5 , 16.5g) and 75.5% polyphosphoric acid (75.5%PPA, 23.5g) were mixed at 150°C under nitrogen atmosphere for 2 hours. After cooling to 120°C, aniline (0.83g, 0.0089mole) and phthalic anhydride (1.33g, 0.0090mole) were added. The reaction mixture was heated to 190°C, and stirred for 4 hours. After the mixture was allowed to cool to room temperature, the product was obtained by pouring the reaction mixture into water, and washed with water several times.

To examine the effects of reaction conditions, the model reaction was carried out at several temperatures and in various compositions of polyphosphoric acid.

Polyimide synthesis in PPA

Under nitrogen atmosphere, P_2O_5 (16.5g) and 75.5% PPA (23.5g) were mixed at 150°C for 2 hours. After the mixture was cooled to 120°C, ODA (0.87g, 0.00434mole) was added and stirring was continued for 30 min. BPDA (1.28g, 0.00435mole) was added and the polymerization was

carried out at 150°C for 3 hours, then at 190°C for 19 hours. After cooled to room temperature, the reaction mixture was mixed with water to precipitate the polymer by using a blender, and the product obtained was washed with water several times.

To examine the effects of reaction conditions, the polymerizations were carried out at several temperatures and in various compositions of polyphosphoric acid.

Poly(imide-benzoxazole) synthesis in PPA

Phosphorus pentoxide (20.02g), 75.5% PPA (24.98), HAB dihydrochloride (1.85g, 0.00644mole) and ABA (1.77g, 0.0129mole) were charged in a reaction vessel, and heating and stirring were started under a nitrogen atmosphere. Keeping the temperature at 90°C, the mixture was evacuated gradually to cause the dehydrochlorination; it took 3 hours to reach ca. 20mmHg. Then, the dehydrochlorination was continued at 150°C for 14 hours. BPDA (1.90g, 0.00646mole) was added, and polymerization was carried out at 200°C for 24 hours. The work-up was made in the same way as that of the polyimide synthesis. Yield was 90%. Anal. Calcd. for $C_{42}H_{20}N_4O_6$: C, 74.55; H, 2.98; N, 8.28. Found (after correction of 2.9wt% of adsorbed moisture): C, 74.45; H, 3.09; N, 8.32.

Poly(imide-benzoxazole) synthesis in organic solvent

The diamine made from HAB and 2 moles of ABA was prepared using the same method as the first half of the procedure for poly(imide-benzoxazole) polymerization in PPA. The reaction mixture was poured into water, and the diamine obtained was washed with water, neutralized with sodium bicarbonate, and washed with water again. 1H -NMR (DMSO- d_6) δ =6.0 (s, 4H, NH_2), 6.7 (d, 4H, aromatic H), 7.7 (s, 4H, aromatic H), 7.9 (d, 4H, aromatic H), 8.0 (s, 2H, aromatic H). Anal. Calcd. for $C_{26}H_{18}N_4O_2$: C, 74.63%; H, 4.34%; N, 13.39%. Found (after correction of adsorbed moisture): C, 74.97%; H, 4.12%; N, 13.27%.

The diamine prepared (1.86g, 0.00444mole) was dissolved in 30ml of NMP under nitrogen atmosphere. BPDA (1.31g, 0.00445mole) was added and stirred for 4 hours. The polyamic acid solution was cast on a glass plate and placed in an oven to imidize thermally at 100°C, 200°C, and 300°C for 1 hour, respectively.

One-pot polymerization and imidization were examined by the addition of 5 drops of isoquinoline into the polyamic acid solution and stirring at 170°C for an additional 3 hours. The viscous turbid reaction mixture was cooled to room temperature and poured into 300ml of methanol. The product was collected by filtration, washed with methanol and dried. Yield was 94%.

The one-pot polymerizations in *m*-cresol and *o*-chlorophenol were carried out in the same manner as the reaction in NMP.

Analysis

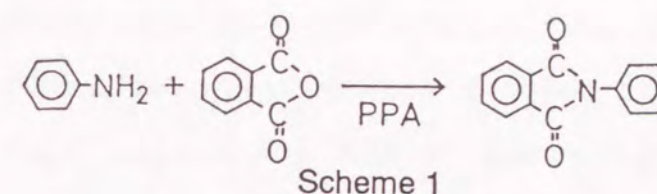
Inherent viscosities of the polymers were measured at a concentration of 0.5g/dl in concentrated sulfuric acid at 30°C. Infrared spectra were measured on a Hitachi 270-30 infrared spectrometer with samples of KBr pellets or films; the films of polyimides were cast from the *o*-chlorophenol solutions on a glass plate at ca. 50°C, coagulated with acetone and dried under vacuum at room temperature. Thermogravimetric analysis (TGA) was conducted at a heating rate of 10°C/min under flowing air or argon, using a thermogravimetric analyzer (Shimadzu TGA-50). ¹H-NMR spectra were obtained in DMSO-*d*₆ solutions with a Varian Gemini-200 spectrometer.

3-3 Results and Discussion

3-3-1 Model Reaction in PPA

Polyphosphoric acid (PPA) is a series of mixtures of condensed phosphoric acid oligomers of which equilibrium composition is determined by the ratio of phosphorus pentoxide (P₂O₅) to water. It has been reported that the P₂O₅ content of more than 82wt% is necessary to cause the polymerization of PBT and PBO.⁵

Imide-ring formation between aniline and phthalic anhydride in PPA was examined as a model reaction of the preparation of polyimide (Scheme 1). Influence of the



PPA composition was compared by using the PPAs of 75, 80 and 85wt% P₂O₅ content. As the reactant concentration was 5wt%, the P₂O₅ content was decreased by 0.4wt% from the starting content by water formed in the reaction. The reaction was carried out at 160 or 190°C. All the products obtained from the combination of PPA compositions and reaction temperatures described above gave the same IR and NMR spectra as for *N*-phenylphthalimide. No characteristic peaks owing to amide linkage or other substances were detected. The NMR spectrum of the

product obtained by using 85wt% PPA at 190°C is shown in Figure 1 as an example; though couplings of aromatic protons are complex, the signals of 7.4-7.6ppm are assigned to the protons on the phenyl ring from aniline and those of 7.9-8.0ppm are assigned to the protons on the 1,2-phenylene ring. PPA concentration was not so critical for the imide preparation in the range of 75-85 wt% of P₂O₅ content.

The reactions in PPA with 75 or 80wt% P₂O₅ content proceeded in homogeneous solutions. On the other hand, the reactions in PPA with 85wt% of P₂O₅ content induced precipitation of the product. PPA with high content of P₂O₅ seems not to be a good solvent for imide compounds. This is probably due to the low basicity of the imide compounds leading to insufficient protonation on solvation by PPA.

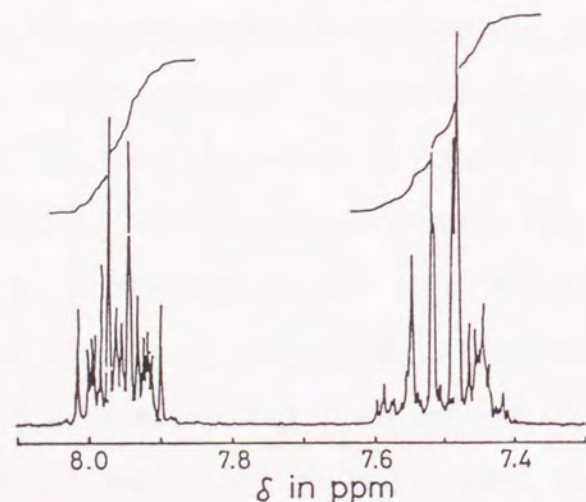


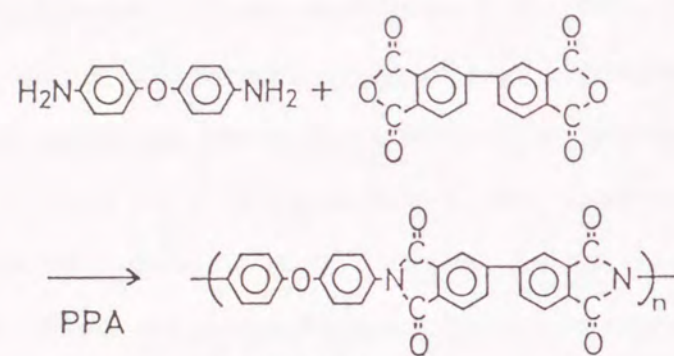
Figure 1. NMR spectrum of *N*-phenylphthalimide prepared in 85wt% PPA at 190°C.

When the reaction was carried out at 220°C in 85wt% PPA, the product changed to a dark color. Too high of reaction temperature induced degradation of the product.

It was reported that synthesis of polyamides and polyesters in PPA was not successful; it was explained by an equilibrium reaction or electrophilic acylation on the benzene ring by carboxyl groups^{14,15}. When *N*-phenylbenzamide was heated in 85wt% PPA at 190°C for 4 hours, the amide absorption in the IR spectrum of the compound disappeared. From these results, it is suggested that a quick dehydrative imide-ring formation from the amic acid is the key to the successful synthesis of the imide compound in PPA.

3-3-2 Synthesis of Polyimide in PPA

The polymerization of ODA and BPDA was carried out at 150°C for 3 hours, thereafter at 190°C for 19 hours in 75, 80, and 85wt% PPA (Scheme 2). The results are summarized in Table I. In all cases, the reaction mixtures became turbid as the reactions proceeded. Higher P₂O₅ content of PPA gave slightly higher inherent viscosity in concentrated sulfuric acid: $\eta_{inh} = 0.90$ dl/g when reacted in 85wt% PPA. Influence of the reaction temperature



Scheme 2

Table I. Polymerization of polyimide in PPA

P ₂ O ₅ content in PPA (wt%)	Reaction temperature (°C)	Yield (%)	η_{inh}^a (dl/g)
75	190	92	0.52
80	190	93	0.77
85	190	93	0.90

^a Measured in concentrated sulfuric acid at 30°C.

Table II. Polymerization of polyimide in 85wt% PPA

P ₂ O ₅ content in PPA (wt%)	Reaction temperature (°C)	Yield (%)	η_{inh}^a (dl/g)
85	160	105	0.04
85	190	93	0.90
85	220	99	1.43

^a Measured in concentrated sulfuric acid at 30°C.

was examined in 85wt% PPA as shown in Table II. The polymerization at 160°C gave a product with a low inherent viscosity, and the IR spectrum showed the absorptions of unreacted anhydride. In the case of polyimide synthesis, it seems that highly dehydrative conditions are necessary to induce the reaction as compared with the model reaction. When polymerized at 220°C, the polymer with an inherent viscosity of 1.43 dl/g was obtained. However, this polymer contained a fraction which did not dissolve in *o*-chlorophenol. Side reactions including crosslinking were suggested at a higher polymerization temperature. The polymerization at 190°C gave a suitable polymer with a relatively high molecular weight and no side reaction.

The IR spectrum of the polymer obtained at 190°C in

85wt% PPA is shown in Figure 2(A). It shows imide absorptions at 1780, 1720, and 1380 cm^{-1} , and is almost identical with the ODA/BPDA polyimide polymerized in NMP and thermally imidized after the cast (Figure 2(B)). No absorption due to the amide bond was detected, and it was ascertained that both the polymerization and imidization were completed under this reaction condition. The polymer prepared in PPA was dissolved in *o*-chlorophenol and converted to a tough and flexible film by casting.

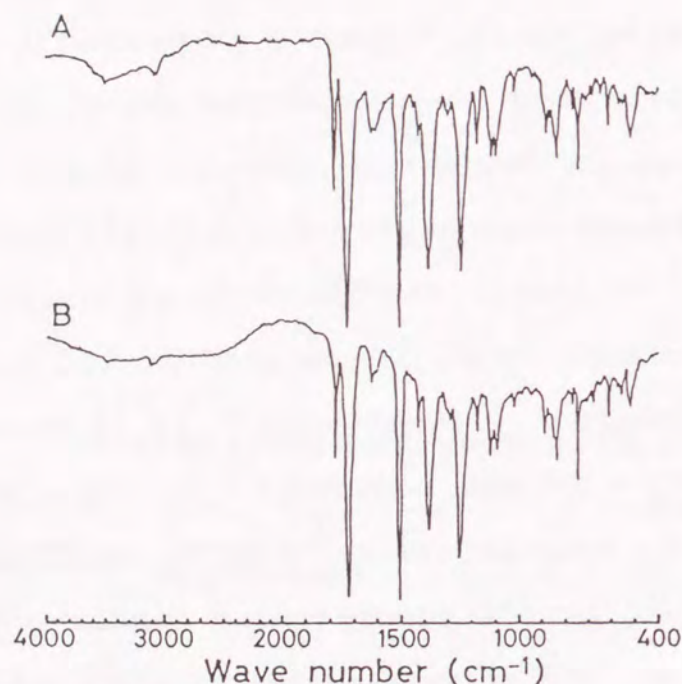
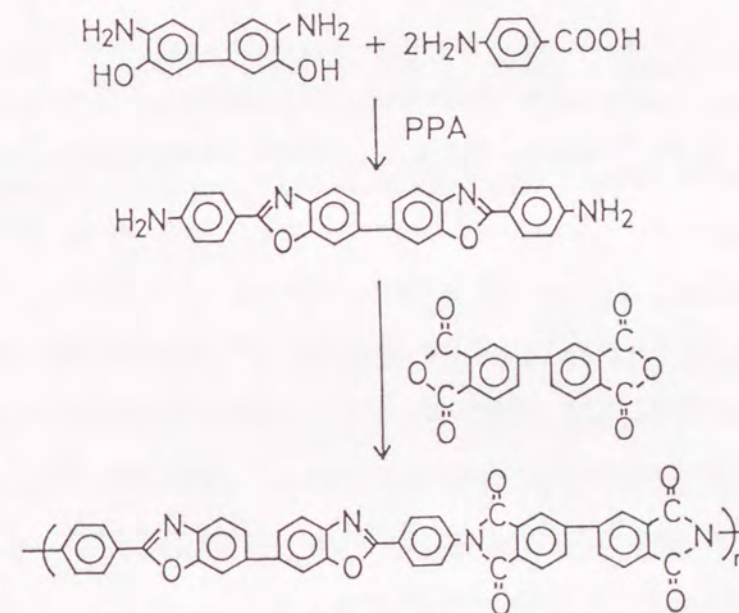


Figure 2. IR spectra of ODA/BPDA polyimide: A, prepared in 85wt% PPA at 190°C; B, polymerized in NMP and thermally imidized.

3-3-3 Synthesis of Poly(imide-benzoxazole) in PPA

3,3'-Dihydroxy-4,4'-diaminobiphenyl dihydrochloride ($\text{HAB} \cdot 2\text{HCl}$) and two moles of 4-aminobenzoic acid (ABA) were reacted in 85.5% PPA to obtain a diamine containing benzoxazole rings. Following this reaction, an equivalent molar amount of BPDA with the diamine was added, and reacted at 200°C for 24 hours (scheme 3). This reaction



Scheme 3

decreased the P_2O_5 content in PPA from 85.5% to 84%. when the reaction proceeded, the solution became viscous and maintained its transparency. The poly(imide-benzoxazole) obtained had an inherent viscosity of 0.59 dl/g. As shown in Figure 3(A), IR spectrum showed imide peaks at 1780, 1720, and 1360 cm^{-1} , and oxazole peaks at 1620,

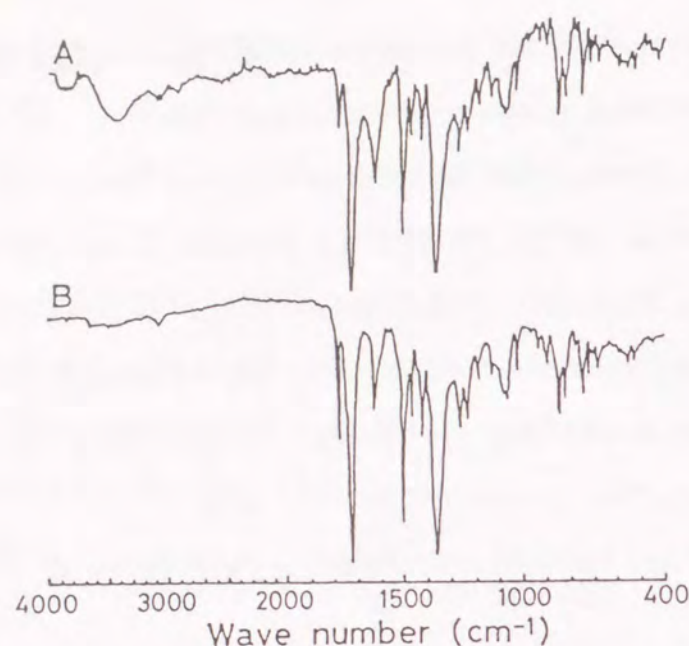


Figure 3. IR spectra of the poly(imide-benzoxazole): A, prepared in PPA; B, polymerized in NMP and thermally imidized.

1260, and 1060 cm^{-1} . The result of elemental analysis is also in good agreement with the calculated values. Poly(imide-benzoxazole) showed high thermal stability with 5% weight-loss temperatures of 559°C in argon and 478°C in air as shown in Figure 4.

As a comparison, the diamine isolated from the PPA reaction was reacted with BPDA in NMP. The polyamic acid solution was cast on a glass plate, and imidized in an oven at 100°C , 200°C , and 300°C for 1 hour, respectively. The poly(imide-benzoxazole) film showed an identical IR spectrum with that of poly(imide-benzoxazole) prepared in PPA (Figure 3(B)).

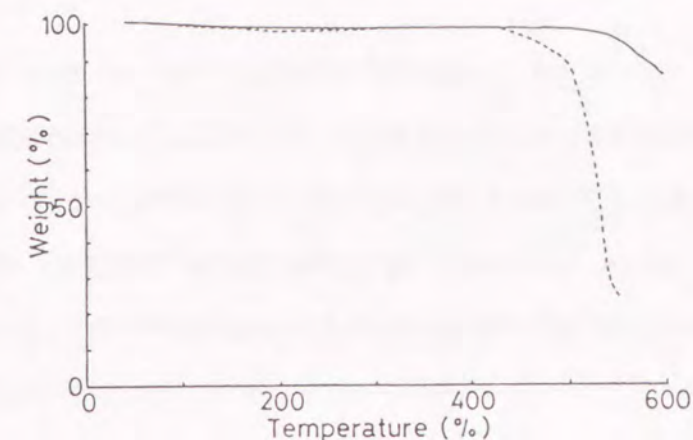


Figure 4. Thermogravimetric curves for the poly(imide-benzoxazole) in argon (solid line) and air (broken line).

The one-pot polymerizations of the diamine and BPDA followed by thermal imidization in NMP, *m*-cresol and *o*-chlorophenol gave poly(imide-benzoxazole) having inherent viscosities of 0.71, 0.59, and 1.26 dl/g , respectively. Although these polymers showed identical IR spectra with that of the polymer prepared in PPA, precipitation occurred during the polymerization, and no homogeneous solution was obtained in contrast to the polymerization in PPA.

As polyimides and polybenzoxazoles show low solubilities in common organic solvents, poly(imide-benzoxazole) did not dissolve in NMP, *m*-cresol or *o*-chlorophenol. On the other hand, affinity of the benzoxazole units for PPA made poly(imide-benzoxazole) soluble in PPA.

The processes of making fibers and films from the poly(imide-benzoxazole) solution in PPA essentially do

not have problem of volatile formation or the incompleteness of dehydrative cyclization, which is sometimes found in the process starting from polyamic acid solutions. Therefore, this polymer has the possibility to be a new processable high-performance polymer.

3-4 Conclusions

The polyimide was synthesized from ODA and BPDA in PPA. In the combinations of PPA composition and reaction temperature, the polymerization in 85wt% PPA at 190°C gave the best result: $\eta_{inh} = 0.90$ dl/g, with no side reactions and film formability. However, the polymer precipitated out during the reaction.

By using the imide-formation reaction in PPA, poly(imide-benzoxazole) was synthesized from HAB, ABA, and BPDA by one-pot polymerization in PPA. The polymer was obtained as a homogeneous solution in PPA, and showed η_{inh} of 0.58 dl/g. As this polymer was not prepared as a homogeneous solution in organic solvents, this system has a possibility as a new processable high-performance polymer solution.

References

1. M.I.Bessonov, M.M.Koton, V.V.Kudryavtsev and L.A.Laius, "Polyimides — Thermally Stable Polymers", Plenum, New York(1987)
2. H.H.Yang, "Aromatic High-strength Fibers", P.673, Wiley Interscience, New York(1989)
3. T.Takekoshi, *Advances in Polym. Sci.*, 94, 1 (1990)
4. Y.Iwakura, *Kobunshi*, 17, 130(1968)
5. J.F.Wolfe, "Encyclopedia of Polymer Science and Technology", 2nd Ed., Vol. 11, P.601, John Wiley and Sons, New York(1988)
6. Y.Iwakura, K.Uno and Y.Imai, *J. Polym. Sci. Part A*, 2, 2605(1964)
7. P.M.Hergenrother, W.Wrasidlo and H.H.Levine, *J. Polym. Sci. Part A*, 3, 1665(1965)
8. Y.Imai, I.Taoka, K.Uno and Y.Iwakura, *Makromol. Chem.*, 83, 167(1965)
9. Y.Imai, K.Uno and Y.Iwakura, *Makromol. Chem.*, 83, 179 (1965)
10. J.F.Wolfe, B.H.Loo and F.E.Arnold, *Macromolecules*, 14, 915(1981)
11. J.F.Wolfe and F.E.Arnold, *Macromolecules*, 14, 909 (1981)
12. Y.Iwakura, K.Uno and T.Takiguchi, *J. Polym. Sci. Part A-1*, 6, 3345(1968)

13. S.Hashimoto and Y.Nagasuna, *Kobunshi Kagaku*, 24, 633(1967)
14. K.Uno, "Gousei To Youkai No Tameno Youbai (*Solvents for Synthesis and Dissolution*)" (Ed. K.Shinoda), Chap.6, P.135, Maruzen, Tokyo(1969)
15. D.A.Denton and H.Suschitzky, *J. Chem. Soc.*, 1963, 4741

Chapter-4

Polymer Structure and Gas Permeability of Poly(sulfone-amide) Membranes : Catenation Effect

4-1 Introduction

Gas separation of small molecules such as hydrogen from larger molecules such as carbon monoxide through stiff-chain glassy-polymer membranes is mainly affected by the packing character of the polymer chains, which determines the diffusivity of the gas molecules.¹

Investigation on the relationship between gas-permeation character and polymer structure has been carried out for years. From these researches, a general concept, that is, aromatic amorphous polymers with high glass transition temperature and stiff-chain structure have a superior permselectivity, was derived to obtain a highly efficient hydrogen separation membrane.² Most of the reports describing the structure-permeability relationships, however, dealt with polymer systems involving several structural factors at the same time, and no systematic research had been published using a series of copolymers until this research was started.

In this chapter, the interest was focused on aromatic polyamides containing sulfone linkages in the backbone [these polymers are called poly(sulfone-amide)]. Aromatic polyamides have stiff-chain structure and relatively high glass transition temperature in general. In addition, sulfone linkages in the poly(sulfone-amide)s contribute to increase their solubility in organic solvents

without sacrificing the structural stiffness.

The purpose of this chapter is to understand the relationship of polymer structure and gas permeability in poly(sulfone-amide)s, especially the catenation effect. Therefore, two series of poly(sulfone-amide) copolymers in which structural difference exists only in *meta/para* ratio were prepared, and the permeabilities of H₂ and CO were evaluated.

4-2 Experimental

Materials

Bis[4-(4-aminophenoxy)phenyl]sulfone (4SED), bis[4-(3-aminophenoxy)phenyl]sulfone (3SED), bis(3-aminophenyl)sulfone (3DDS) (these three monomers were obtained from Konishi Chemical Ind. Co., Ltd.) and bis(4-aminophenyl)sulfone (4DDS) (Wakayama Seika Kogyo Co., Ltd.) were used as purchased. Isophthaloyl chloride (IPC) (Mitsubishi Gas Chemical Co., Inc.) was crushed to a powder under nitrogen atmosphere. *N*-Methyl-2-pyrrolidone (NMP) was dried over molecular sieves more than one day before use.

Polymerization

The diamine components were dissolved in NMP under nitrogen atmosphere, in such a way that the concentration of resulting polymer solution became 20wt%. This solution was cooled below 5°C in an ice bath and then an equimolar amount of IPC was added. After the solution was stirred for an hour in the ice bath, the polymerization was continued for another hour at room temperature. The polymer solution was poured into methanol. The polymer precipitated was washed with water several times by use of a blender, and then dried for a period of one day under reduced pressure at 150°C.

Preparation of Membranes

The polymers (4g) were dissolved in 20ml of NMP. The solutions were filtered and cast on a polypropylene film at room temperature, and the solvent was evaporated at 80°C for an hour. The membrane was dried under reduced pressure at 150°C for 15 hours. Thickness of films obtained was 10 - 20 μm.

Characterization

Reduced viscosities of the polymers were measured at a concentration of 0.5g/dl in *N,N*-dimethylacetamide (DMAc) at 30°C. Glass transition temperatures were

determined by using a differential scanning calorimeter (DSC) (Perkin-Elmer DSC-1B) at a heating and cooling rate of 20°C/min under flowing argon. Thermogravimetric analysis (TGA) was conducted on a thermogravimetric analyzer (Shimadzu TG-30) at a heating rate of 10°C/min under flowing air. ¹H-NMR spectra were measured on Varian Gemini-200 spectrometer using dimethyl sulfoxide-*d*₆ as a solvent. Densities of the membranes were obtained by use of a density gradient column which consisted of *n*-heptane and carbon tetrachloride at 30°C.

Permeability Measurement

Permeabilities of H₂ and CO were measured with a permeation apparatus made by Rika Seiki Kogyo, and MKS Baratron pressure transducer was used for detection of pressure increase in the downstream gas reservoir. Gas samples of purity exceeding 99.9% were used.

In order to analyze gas permeation through a glassy polymer in detail, consideration based on the dual-mode theory³ is necessary. However, many papers discuss data on the permeation and sorption measurements under a certain pressure, and give useful information on the molecular design of gas separation membranes. There are also articles describing agreement between solubility data from sorption experiment and those calculated from

the time-lag method for some polymers. The purpose of this research is to obtain information about the molecular design for gas separation membranes.

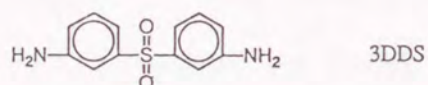
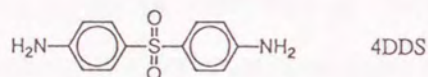
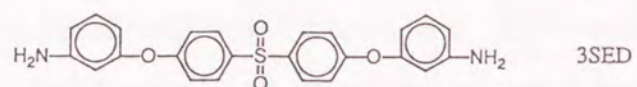
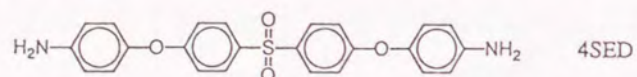
From these reasons, the permeability coefficient was determined from the steady-state permeation rate at a constant pressure of upstream gas (1 atm), and the apparent diffusion coefficient of CO was determined using the time-lag method.⁴ The apparent diffusion coefficient (*D*_{app}) was calculated by the following equation,

$$D_{app} = \frac{l^2}{6L}$$

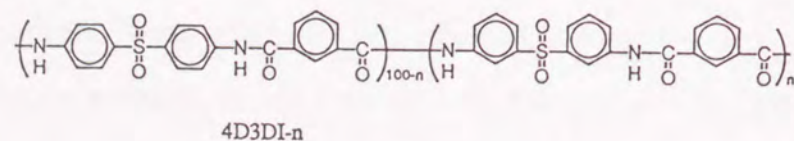
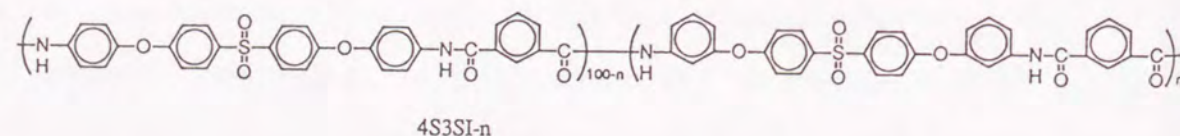
where *L* is the time lag, and, *l*, the thickness of the membrane. The permeation of H₂ was too fast to determine the time lag accurately, and the apparent diffusion coefficient of H₂ was not evaluated.

4-3 Results and Discussion

Poly(sulfone-amide) copolymers were prepared to clarify the relationships between polymer structure and gas permeability from view point of the influence of catenation. For this purpose, four diamines shown below were selected to polymerize with isophthaloyl chloride (IPC); 4SED and 3SED contain ether and sulfone linkages, 4DDS and 3DDS contain only the sulfone linkage and give a polymer with a higher fraction of amide linkages.



The structural formulas of two series of poly(sulfone-amide) copolymers obtained from these monomers are shown below.



4-3-1 Preparation and Properties of Poly(sulfone-amide)s

The results of preparation and some characterizations of copolymers are shown in Table I. Each polymer had a reduced viscosity sufficient to give a tough membrane. The polymer composition was determined by ^1H -NMR spectroscopy. As an example, ^1H -NMR spectrum of the polymer 4S3SI-50 is shown in Figure 1. The polymer composition measured was almost the same as the monomer composition for every polymer sample. Each polymer had a high glass transition temperature above 200°C , and 4D3DI series showed the glass transition ca. 50°C higher than the corresponding 4S3SI series. They showed similar thermal stabilities with the 5% weight-loss temperatures above 400°C in air.

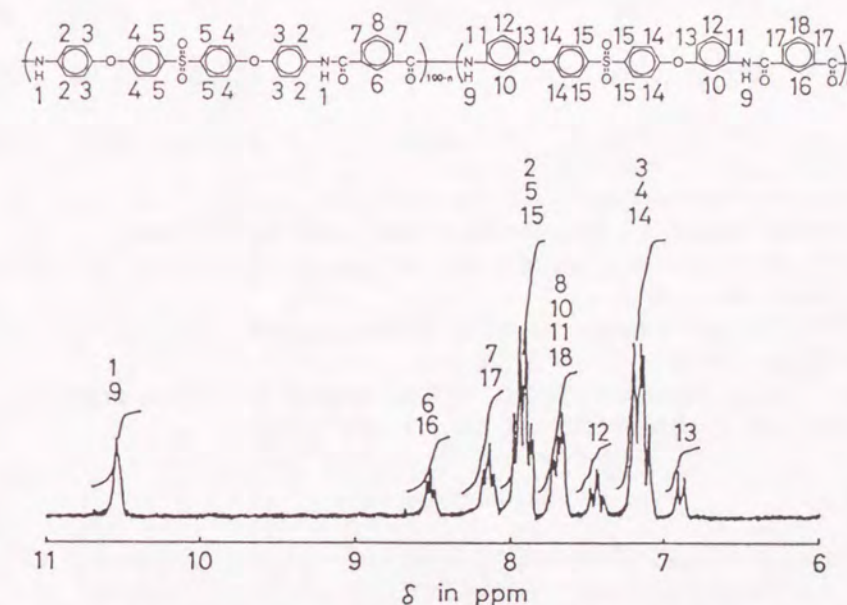


Figure 1. ^1H -NMR spectrum of 4S3SI-50 in $\text{DMSO}-d_6$

Table I. Preparation and properties of Poly(sulfone-amide) Copolymers

polymer	Monomer Ratio (molar ratio)		3SED or 3DDS ^a Content in Polymer (mol%)	η_{sp}/C^b (dl/g)	T_g^c (°C)	TGA ^d (°C)
	4SED	3SED	3SED			
4SI	100	0	0	1.25	261	443
4S3SI-25	75	25	27	0.89	250	447
4S3SI-50	50	50	51	0.67	236	447
4S3SI-75	25	75	74	0.65	230	440
3SI	0	100	100	0.46	210	441
	4DDS	3DDS	3DDS			
4DI	100	0	0	0.77	322	439
4D3DI-25	75	25	25	0.66	307	418
4D3DI-50	50	50	49	1.13	292	415
4D3DI-75	25	75	74	1.15	278	408
3DI	0	100	100	1.01	264	455

a 3SED or 3DDS unit content determined by $^1\text{H-NMR}$.

b Reduced viscosity measured at a concentration of 0.5 g/dl in DMAc at 30°C.

c Glass transition temperature determined by DSC in argon at a heating rate of 20°C/min.

d 5% weight loss temperature determined by thermogravimetry in air at a heating rate of 10°C/min.

4-3-2 Gas Permeability of Poly(sulfone-amide) Copolymers

The permeability coefficients (P) of H_2 and CO through 4S3SI and 4D3DI copolymers at 30°C are illustrated in Figure 2. The permeabilities of both gases decreased monotonously with an increase in *meta*-diamine content in each copolymer system. The apparent diffusion coefficient ($D_{app.}$) of CO also decreased with increasing *meta*-diamine content (Figure 3), and these orders were in good agreement with the order of density of membranes as shown in Table II.

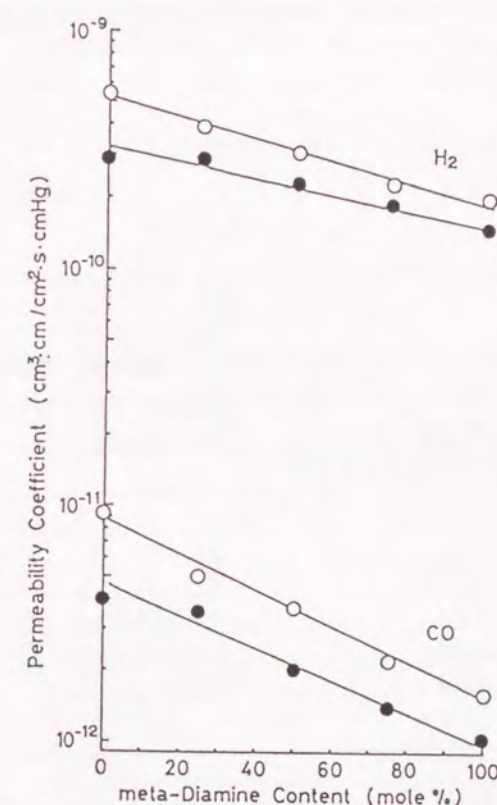


Figure 2. Relation between permeability coefficients and composition of the poly(sulfone-amide) copolymers: ○, 4S3SI copolymers; ●, 4D3DI copolymers.

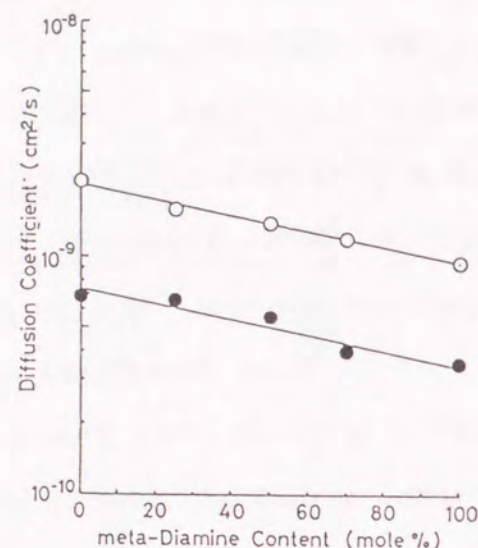


Figure 3. Relation between diffusion coefficient for CO and composition of the poly(sulfone-amide) copolymers: ○, 4S3SI copolymers; ●, 4D3DI copolymers.

Table II. Density of the poly(sulfone-amide) membranes

Polymer	Density* (g/cm ³)	Polymer	Density* (g/cm ³)
4SI	1.321	4DI	1.360
4S3SI-25	1.322	4D3DI-25	1.360
4S3SI-50	1.323	4D3DI-50	1.361
4S3SI-75	1.326	4D3DI-75	1.362
3SI	1.328	3DI	1.362

* Density measured at 30°C with a density gradient column.

Diffusivity is usually discussed on the basis of packing character: chain packing from free volume analysis, intersegmental spacing from X-ray diffraction, chain stiffness with consideration of segmental mobility, and so on. The packing density is defined by the following equation^{5,6}:

$$\text{Packing Density} = \frac{\text{Specific Volume}}{(\text{Specific Volume} - \text{Specific van der Waals Volume})}$$

Here, specific van der Waals volume was obtained by using a computer program system "MOL-GRAPH", Daikin Industries, Ltd. The relation between packing density and CO diffusivity is shown in Figure 4. It indicates that the

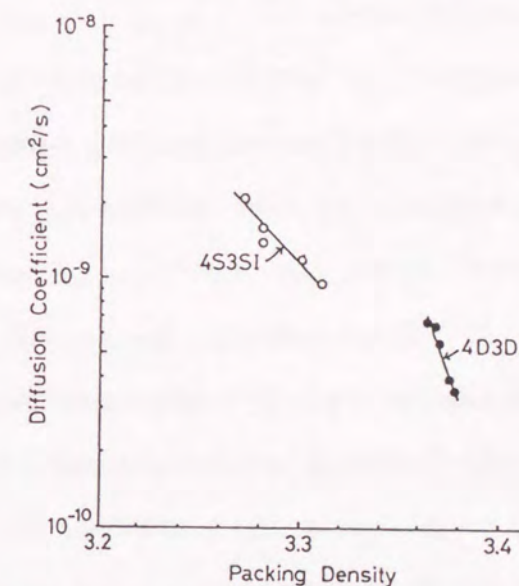


Figure 4. Correlation between packing density and diffusion coefficient for CO in the poly(sulfone-amide) copolymers.

existence of *m*-catenation contributes to the compact packing of the polymer chains more effectively than that of *p*-catenation. This effect may be induced by the conformational freedom enhanced by *m*-catenation during the formation of membrane structure.⁷

Although definite conclusions about the solubility coefficient should not be discussed based on these measurements, the decrease in the apparent solubility coefficient for CO ($S_{app.CO}$) with an increase in *meta*-diamine content was found in both copolymer systems from the calculation using the relation of $S_{app.} = P / D_{app.}$. As the difference in the chemical influence on gas sorption in each copolymer system is negligible, the Langmuir sorption caused by micro voids is suggested as a reason for the solubility change.

When *m*-catenation content increased, permeability of CO decreased more significantly than that of H₂. As a result, the permeability ratio for H₂ relative to CO (P_{H_2}/P_{CO}) increased with the content of *m*-catenation as shown in Figure 5. This effect is mainly induced by a decrease in CO diffusivity, and the influence of the decrease in CO solubility is also suggested at the same time.

It had been considered that stiffer structure in the polymers makes the membrane structure more compact and restricts the gas diffusion. Therefore, the catenation

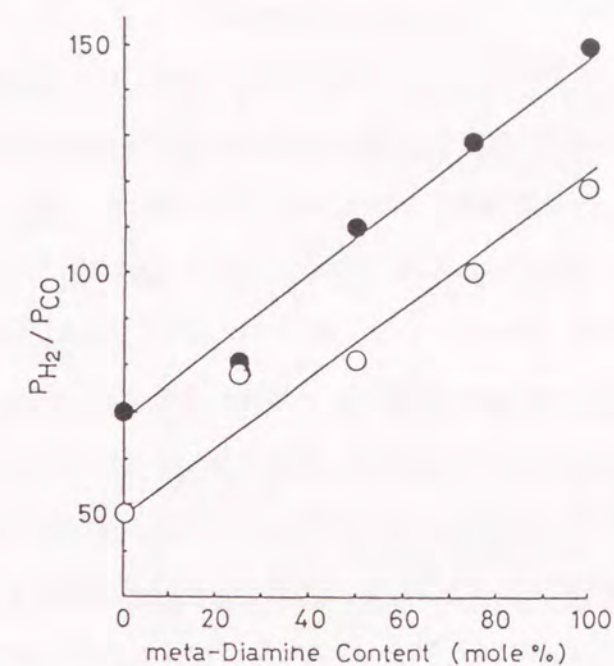


Figure 5. Relation between permeability ratio for H₂ relative to CO at 30°C and composition of the poly-(sulfone-amide) copolymers: O, 4S3SI copolymers; ●, 4D3DI copolymers.

effect found in this work was an unexpected one because the *m*-catenation makes the polymer chain more flexible. This interesting effect has recently been reported for some other polymers.⁷⁻¹²

All the 4D3DI copolymers showed lower gas permeabilities as compared with the corresponding 4S3SI copolymers. Though these results suggest the existence of an effect of chain-stiffness enhanced with an increase in amide-linkage fraction, this effect will be discussed in next chapter.

4-4 Conclusions

Two series of poly(sulfone-amide) copolymers in which the catenation structure was changed systematically were prepared, and gas permeabilities of H₂ and CO were examined. The polymers containing higher fractions of *m*-linkages showed lower gas permeabilities for both the gases and a higher permselectivity of H₂ relative to CO. This effect was explained by the restriction of gas diffusion caused by the denser structure of the polymers with high *meta/para* ratios, especially for a larger gas species such as CO. The gas diffusivity showed good agreement with the tendency of packing density estimated from the free volume.

References

1. T.Nakagawa, *Energy Shigen*, 6, 258(1985)
2. F.P.McCadless, *Ind. Eng. Chem. Process Des. Develop.*, 11, 470(1972)
3. W.J.Koros and D.R.Paul, *J. Polym. Sci., Polym. Phys. Ed.*, 14, 675(1976)
4. R.M.Barrer, *Trans. Faraday Soc.*, 35, 628(1939)
5. R.T.Chern, F.R.Sheu, L.Jia, V.T.Stannett and H.B. Hopfenberg, *J. Membr. Sci.*, 35, 103(1987)
6. F.R.Sheu, R.T.Chern, V.T.Stannett and H.B. Hopfenberg, *J. Polym. Sci., Polym. Phys. Ed.*, 26, 883(1988)
7. K.Tanaka, H.Kita, K.Okamoto, A.Nakamura and Y.Kusuki, *Polym. J.*, 22, 381(1990)
8. G.F.Sykes and A.K.St.Clair, *J. Appl. Polym. Sci.*, 32, 3725(1986)
9. S.A.Stern, Y.Mi, H.Yamamoto and A.K.St.Clair, *J. Polym. Sci., Polym. Phys. Ed.*, 27, 1887(1989)
10. R.E.Kesting, A.K.Fritzsche, M.K.Murphy, C.A.Cruse, A.C.Handermann, R.F.Malon and M.D.Moore, *J. Appl. Polym. Sci.*, 40, 1557(1990)
11. K.Tanaka, H.Kita and K.Okamoto, *Kobunshi Ronbunshu*, 47, 945(1990)
12. F.P.Sheu and R.T.Chern, *J. Polym. Sci., Polym. Phys. Ed.*, 27, 1121(1989)

Chapter-5

Polymer Structure and Gas Permeability

of

Poly(sulfone-amide) Membranes

: Effect of Amide-Linkage Concentration

5-1 Introduction

To separate small molecules such as hydrogen from larger molecules such as carbon monoxide through glassy-polymer membranes, it had been said that aromatic amorphous polymers with high glass transition temperature and stiff-chain structure have a superior permselectivity.¹ In chapter 4, however, it was found that membranes of the poly(sulfone-amide)s containing higher fractions of *m*-linkages, which make the polymer structure flexible, could form a compact structure and restrict gas diffusion more effectively.

In Chapter 4, another structural effect was discussed, that is, the polymers having high amide-linkage concentrations in their backbone reduced gas diffusivity. Amide linkage makes the polymer chain stiff and raise the glass transition temperature. It may also form intermolecular hydrogen bonding so that the membrane structure could become more compact. Therefore, the effect of amide-linkage concentration is in agreement with the effect expected from conventional thoughts.

In this chapter, to clarify the effect of the amide-linkage concentration, series of poly(sulfone-amide) copolymers comprising mixed diamines having different molecular sizes were prepared, and their gas permeabilities were compared. A hybrid effect of catenation and

amide-linkage concentration was also considered.

5-2 Experimental

Materials

m-Phenylenediamine (MPD, Nacalai Tesque) was distilled under reduced pressure and ground to a powder under nitrogen atmosphere. *p*-Phenylenediamine (PPD, Nacalai Tesque) was ground to a powder under nitrogen atmosphere. Other reagents were used as described in chapter 4.

Polymerization

Poly(sulfone-amide)s were prepared by low-temperature solution polycondensation and cast into films as described in Chapter 4.

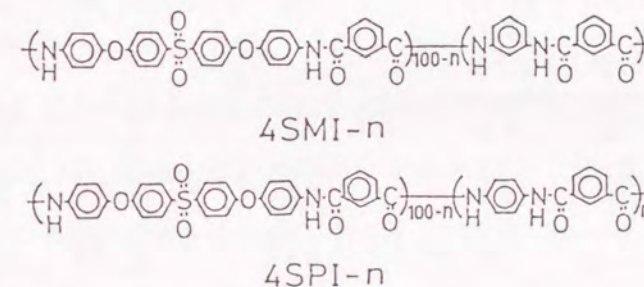
Measurements

Permeabilities of H₂ and CO, and other properties were measured as described in chapter 4.

5-3 Results and Discussion

5-3-1 Gas Permeability of Poly(sulfone-amide) Copolymers Derived from 4SED and Phenylenediamines

To investigate the effect of amide-linkage concentration in the polymer backbone on the gas permeabilities for H₂ and CO, the poly(sulfone-amide) copolymers derived from isophthaloyl chloride (IPC) and mixed diamines which consisted of various ratios of bis[4-(4-aminophenoxy)-phenyl]sulfone (4SED) and *m*-phenylenediamine (MPD) or *p*-phenylenediamine (PPD) were prepared. The polymer structures are shown below, and abbreviated as 4SMI and 4SPI series, respectively.



The results of preparation and some characterizations are summarized in Table I. The polymer composition was determined by ¹H-NMR spectroscopy. As an example, ¹H-NMR spectrum of the polymer 4SMI-60 is shown in Figure 1. The polymer composition measured was almost the same as the monomer composition for every polymer sample. The glass transition temperature increased with phenylenedia-

Table I. Preparation and Properties of Poly(sulfone-amide) Copolymers

Polymer	Monomer Ratio (molar ratio)		4SED-unit ^a Content in Polymer (mol%)	η_{sp}/C^b (dl/g)	T_g^c (°C)	TGA ^d (°C)
	4SED	MPD				
4SI	100	0	100	1.25	261	443
4SMI-05	95	5	96	1.03	261	430
4SMI-15	85	15	84	1.02	262	419
4SMI-25	75	25	72	1.01	263	412
4SMI-35	65	35	64	1.02	263	416
4SMI-45	55	45	54	0.95	264	428
4SMI-60	40	60	42	1.29	263	429
4SMI-70	30	70	33	1.20	267	436
	4SED	PPD				
4SPI-05	95	5	94	1.13	264	426
4SPI-15	85	15	84	1.54	265	422
4SPI-25	75	25	74	1.13	267	409
4SPI-35	65	35	65	1.28	269	429
4SPI-45	55	45	54	2.07	278	427

a 4SED-unit content determined by ^1H -NMR.

b Reduced viscosity measured at a concentration of 0.5 g/dl in DMAc at 30°C.

c Glass transition temperature determined by DSC in argon at a heating rate of 20°C/min.

d 5% weight loss temperature determined by thermogravimetry in air at a heating rate of 10°C/min.

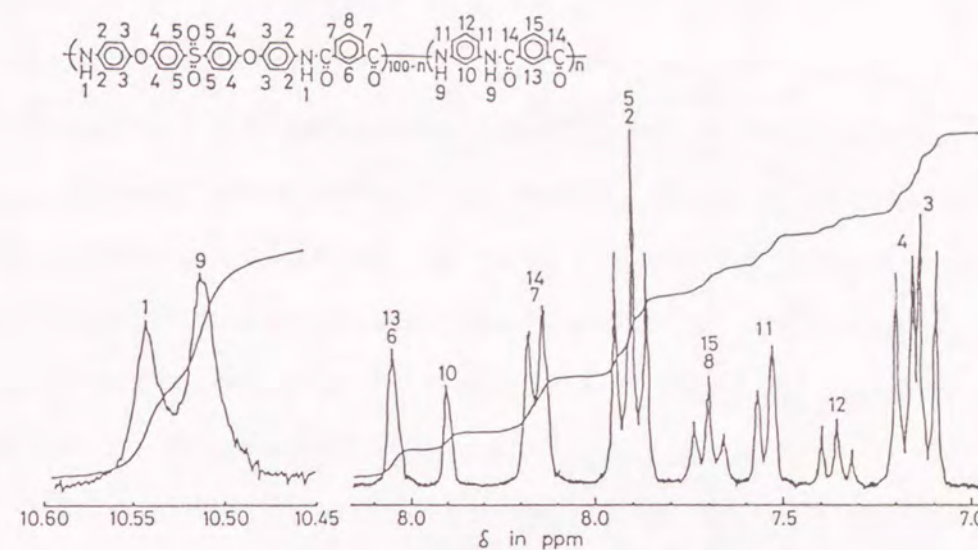


Figure 1. ^1H -NMR spectrum of 4SMI-60 in $\text{DMSO}-d_6$.

mine content, and 4SPI series showed higher glass transition temperatures than the corresponding 4SMI series. They showed similar thermal stability with the 5% weight-loss temperature above 400°C in air. Solubility of the polymers in NMP decreased with an increase of the MPD or PPD content, more remarkable in 4SPI series.

The permeability coefficients (P) of H_2 and CO through both copolymer systems at 30°C are illustrated in Figure 2. The permeabilities of both gases decreased monotonously with an increase in the phenylenediamine content in each copolymer system. Figure 3 shows that the apparent diffusion coefficient ($D_{app.}$) of CO also decreased with an increase in the phenylenediamine con-

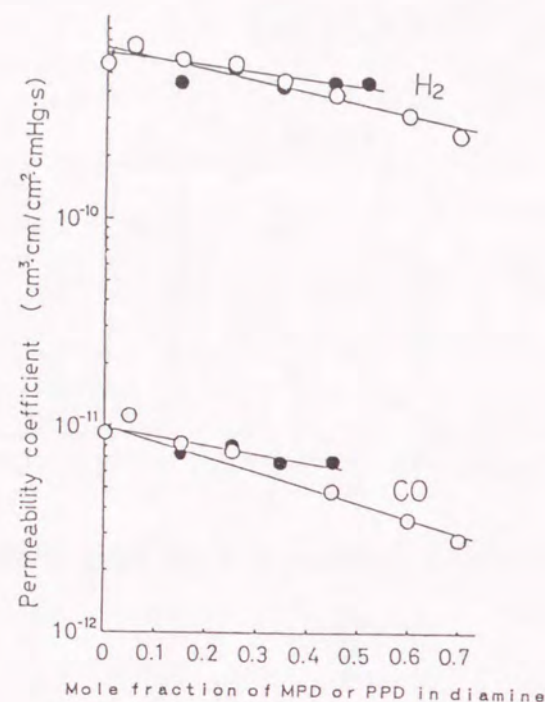


Figure 2. Relation between permeability coefficients and composition of the poly(sulfone-amide) copolymers: ○, 4SMI copolymers; ●, 4SPI copolymers.

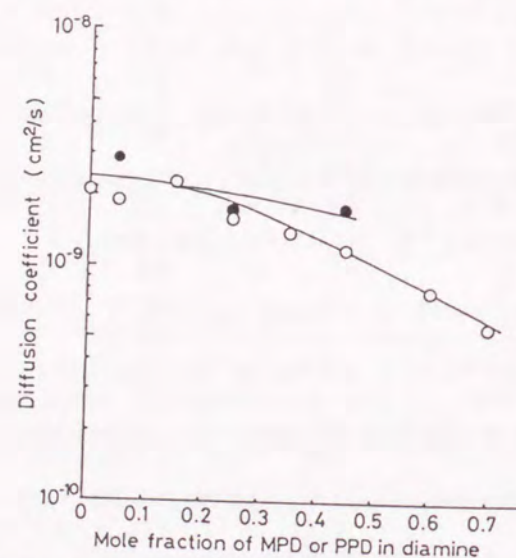


Figure 3. Relation between diffusion coefficient for CO and composition of the poly(sulfone-amide) copolymers: ○, 4SMI copolymers; ●, 4SPI copolymers.

tent. The calculated solubility coefficients ($S_{app.}$) were scattered in the range of 1.4×10^{-3} and $1.9 \times 10^{-3} \text{ cm}^2/\text{s}$, and no definite relationship between P_{CO} and $S_{app.CO}$ was obtained. Therefore, it is considered that the permeation of CO is controlled by the diffusion characteristics. It was also confirmed that $D_{app.CO}$ had a good correlation with the packing density calculated in the same manner as Chapter 4^{2,3} (Figure 4).

From these results, it was found that an increase in the amide-linkage concentration contributed to the densification of membrane structure. As diffusion of larger molecules such as CO is restricted more significantly when membrane structure becomes denser, permselectivity P_{H_2}/P_{CO} increased with increasing phenylenediamine content in both the copolymer systems as shown in Figure 5.

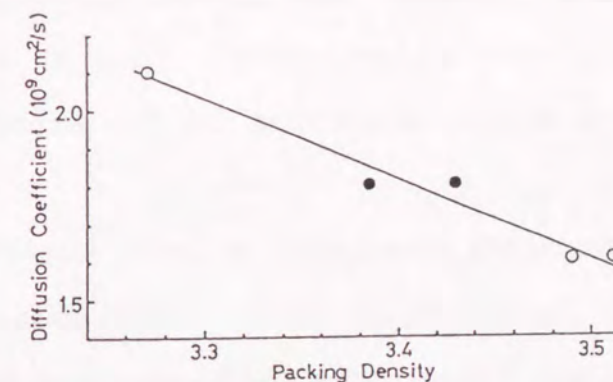


Figure 4. Correlation between packing density and diffusion coefficient for CO in the poly(sulfone-amide) copolymers: ○, 4SMI copolymers; ●, 4SPI copolymers.

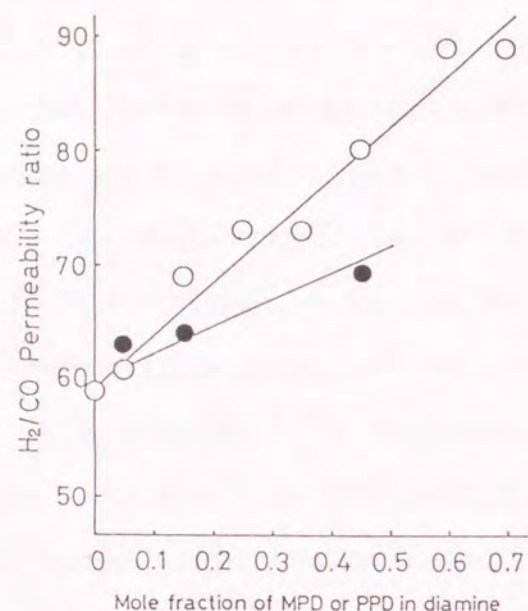


Figure 5. Relation between permeability ratio for H₂ relative to CO at 30°C and composition of the poly-(sulfone-amide) copolymers: ○, 4SMI copolymers; ●, 4SPI copolymers.

Compared with 4SPI copolymers, 4SMI series had more compact membrane structure, and showed lower gas permeability and higher permselectivity. This is attributed to the catenation effect described in the previous chapter.

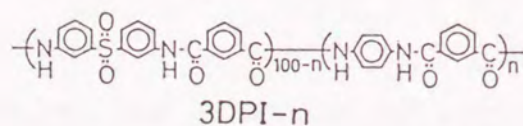
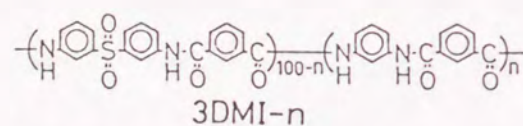
Though the packing densities of 4SMI and 4SPI copolymers with high content of phenylenediamines showed higher values than those of 4D3DI copolymers, the CO permeability of 4SMI and 4SPI copolymers was not lower than that of 4D3DI copolymers. This suggests that the

gas diffusivity of poly(sulfone-amide) membranes was influenced by not only the packing density but also other effects such as segmental motion. For example, 4SMI and 4SPI copolymers have relatively higher content of *p*-phenylene units which can rotate without any other conformational changes in the main chains,⁴ and this rotation may increase the gas diffusivity. Therefore, the packing density should not be used as a general standard to elucidate the gas diffusivity for many kinds of polymers, though it is useful to compare the gas diffusivity in a series of copolymers.

5-3-2 Gas permeability of Poly(sulfone-amide) Copolymers Derived from 3DDS and Phenylenediamines

The poly(sulfone-amide) copolymers comprising bis(3-aminophenyl)sulfone (3DDS) as a main diamine component were examined next. 3DDS has no ether linkage, so the poly(sulfone-amide)s comprising 3DDS has a higher concentration of amide linkages in the main chain than those comprising 4SED. Moreover, the amino groups of 3DDS are bonded on the *m*-position. High permselectivity is expected from these features.

Mixed diamines consisting of various ratios of 3DDS and *m*-phenylenediamine (MPD) or *p*-phenylenediamine (PPD) were reacted with isophthaloyl chloride (IPC) to afford poly(sulfone-amide) copolymers. The polymer structures are shown below, and abbreviated as 3DMI and 3DPI series, respectively.



The results of preparation and some characterizations are summarized in Table II. The polymer composition determined by ¹H-NMR spectroscopy was in good agree-

Table II. Preparation and Properties of Poly(sulfone-amide) Copolymers

Polymer	Monomer Ratio (molar ratio)		3DDS-unit ^a Content in Polymer (mol%)	η _{sp} /C ^b (dl/g)	T _g ^c (°C)	TGA ^d (°C)
	3DDS	MPD				
3DI	100	0	100	1.01	264	451
3DMI-15	85	15	82	0.97	264	442
3DMI-30	70	30	69	0.81	266	443
3DMI-50	50	50	51	1.01	266	451
3DMI-70	30	70	29	1.64	271	438
3DMI-80	20	80	21	1.37	275	417
MI	0	100	0	—	308	400
	3DDS	PPD				
3DPI-30	70	30	67	1.31	272	447
3DPI-50	50	50	49	1.07	277	440

a 3DDS-unit content determined by ¹H-NMR.

b Reduced viscosity measured at a concentration of 0.5 g/dl in DMAc at 30°C.

c Glass transition temperature determined by DSC in argon at a heating rate of 20°C/min.

d 5% weight loss temperature determined by thermogravimetry in air at a heating rate of 10°C/min.

ment with the monomer composition for every polymer sample. ^1H -NMR spectrum of the polymer 3DMI-30 is shown in Figure 6 as an example. The glass transition temperature increased with phenylenediamine content, and 3DPI series showed higher glass transition temperatures than the corresponding 3DMI series.

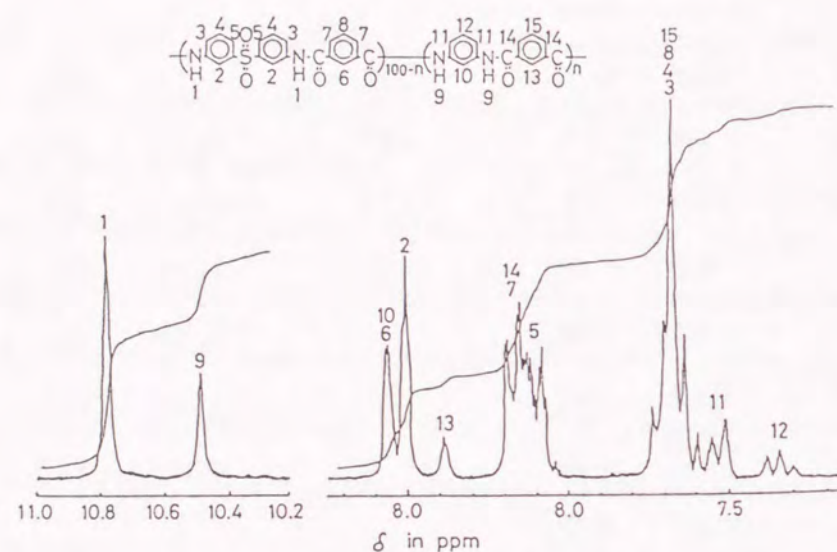


Figure 6. ^1H -NMR spectrum of 3DMI-30 in $\text{DMSO}-d_6$.

The permeability coefficients (P) of H_2 and CO through both copolymer systems at 30°C are illustrated in Figure 7. In 3DPI series, P_{H_2} and P_{CO} increased with an increase in the PPD content in spite of the increase in the amide-linkage concentration. In 3DMI series, P_{CO} decreased with an increase in the MPD content until

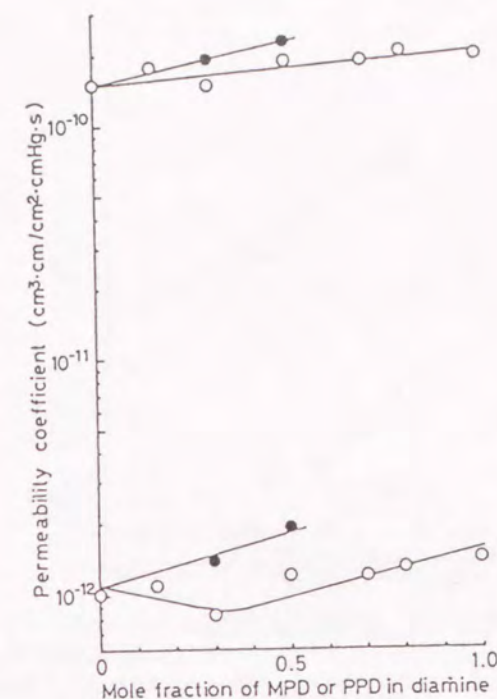


Figure 7. Relation between permeability coefficient and composition of the poly(sulfone-amide) copolymers: \circ , 3DMI copolymers; \bullet , 3DPI copolymers.

30 mol%, and increased with further increase in the MPD content, while P_{H_2} increased monotonously with an increase in the MPD content. As a result, $P_{\text{H}_2}/P_{\text{CO}}$ of 3DMI series showed the maximum value of 185 at the MPD content of 30mol%, and that of 3DPI series decreased monotonously with an increase in the PPD content as shown in Figure 8. Though $P_{\text{H}_2}/P_{\text{CO}}$ of 3DMI copolymers showed scattered results because of small values of P_{CO} , the existence of maximum at 30mol% MPD content was confirmed by repeated experiments. 3DMI-30 has the highest permse-

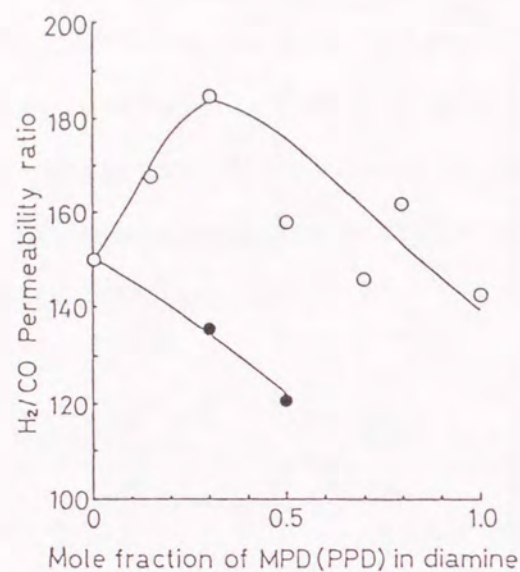


Figure 8. Relation between permeability ratio for H₂ relative to CO at 30°C and composition of the poly(sulfone-amide) copolymers: ○, 3DMI copolymers; ●, 3DPI copolymers.

lectivity in the poly(sulfone-amide) copolymers examined in this research.

A change in the diffusion coefficient of CO ($D_{app.CO}$) with polymer composition was similar to that of P_{CO} as shown in Figure 9. Therefore, the gas permeability of these copolymers was controlled by gas diffusivity, not by solubility. Figure 10 also shows that P_{H_2}/P_{CO} was determined by diffusivity change.

As the poly(sulfone-amide) derived from 3DDS (3DI) contained high *m*-catenation content and amide-linkage concentration, it showed relatively high permselectivity.

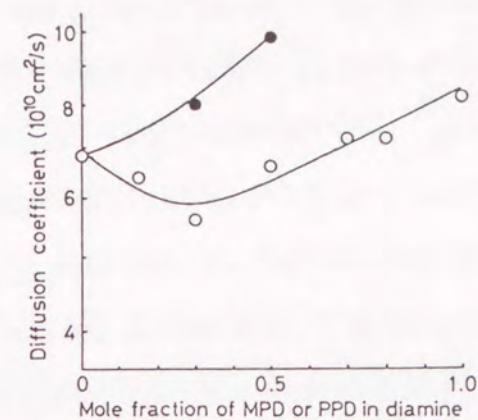


Figure 9. Relation between diffusion coefficient for CO and composition of the poly(sulfone-amide) copolymers: ○, 3DMI copolymers; ●, 3DPI copolymers.

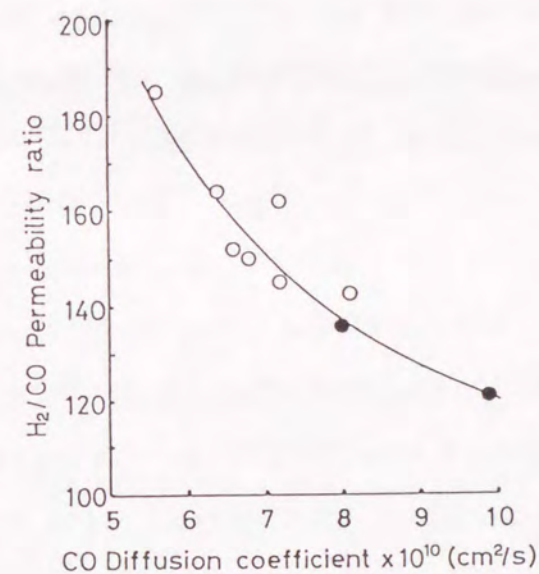


Figure 10. Relation between permeability ratio for H₂ relative to CO and diffusion coefficient for CO of the poly(sulfone-amide) copolymers at 30°C: ○, 3DMI copolymers; ●, 3DPI copolymers.

When copolymerized with PPD, though amide-linkage concentration increased, the polymer structure became too stiff to form a denser membrane. When copolymerized with MPD, small amount of MPD content contributed to the formation of denser membranes, and further copolymerization made the polymer chain too stiff despite increasing *m*-catenation fraction. The advantage of appropriate flexibility in the backbone to give a dense membrane is attributed to a conformational freedom during formation of membrane structure.

From these results including those of Chapter 4, it is concluded that the gas permeability of poly(sulfone-amide) is controlled by the balance between the effect of catenation and the effect of amide-linkage concentration; the former increases the flexibility of the polymer chain and the latter increases the stiffness.

5-4 Conclusions

Four series of poly(sulfone-amide) copolymers in which the amide-linkage concentration in the backbone was changed systematically were prepared, and gas permeabilities of H₂ and CO were examined. When the amide-linkage concentration increased, the gas permeability decreased and permselectivity of H₂ relative to CO increased. However, too high a concentration of the amide linkage induced an increase in the permeability and a decrease in the permselectivity. There was the composition which showed the maximum permselectivity. These characteristics of gas permeation were explained by the gas diffusivity which was related to the packing character of the polymer chains. The catenation effect described in Chapter 4 was also confirmed in these copolymers. As a result, the 3DMI-30 membrane showed the highest H₂/CO permselectivity with $P_{H_2}/P_{CO} = 185$ in the poly(sulfone-amide) copolymers. Therefore, it is concluded that the gas permeability of poly(sulfone-amide)s is mainly determined by the packing character which is controlled by the balance between the stiffness enhanced by the amide linkage and the flexibility induced by the catenation effect.

References

1. F.P.McCadless, *Ind. Eng. Chem. Process Des. Develop.*, 11, 470(1972)
2. R.T.Chern, F.R.Sheu, L.Jia, V.T.Stannett and H.B.Hopfenberg, *J. Membr. Sci.*, 35, 103(1987)
3. F.R.Sheu, R.T.Chern, V.T.Stannett and H.B.Hopfenberg, *J. Polym. Sci., Polym. Phys. Ed.*, 26, 883(1988)
4. S.A.Stern, H.Yamamoto and A.K.St.Clair, *J. Polym. Sci., Polym. Phys.*, 27, 1887(1989)

Chapter-6

Changes of Gas Permeability and Membrane Structure of Poly(sulfone-amide)s in the Process of Solvent Removal

6-1 Introduction

Under a certain condition for preparing membranes, the gas permeabilities and permselectivity of the poly(sulfone-amide)s were affected by the polymer composition. The increase in the permeability ratio for H_2 relative to CO (P_{H_2}/P_{CO}) was mainly caused by a decrease in the diffusion coefficient for CO (D_{CO}). Therefore, the permselectivity was correlated to the packing character of the polymer chains. The results obtained in previous chapters showed that P_{H_2}/P_{CO} is controlled by the balance between the stiffness induced by the concentration of amide linkages in the backbone and the crookedness enhanced with the introduction of *m*-catenation into the main chains.

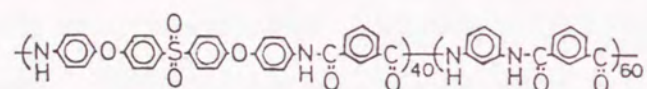
The poly(sulfone-amide) membranes are prepared by the casting from their polymer solutions. The packing character of the polymer chains are changed not only by the polymer structure, but also by the conditions of the membrane preparation. Thermal treatment after the cast induces removal of the cast solvent and rearrangement of the polymer chains, and plays an important role to determine the membrane character. In this chapter, the influence of the process of the solvent removal on the gas permeability and membrane structure was studied. Density measurement was carried out to evaluate the packing

character of the polymer chains, and some analytical methods were used to evaluate structural changes of the membranes. On the basis of the obtained data, relationships between gas permeability and membrane structure are discussed.

6-2 Experimental

Preparation of Polymer

The poly(sulfone-amide) (4SMI-60, structure shown below) was prepared by low-temperature solution condensa-



tion as described in Chapter 4. The reduced viscosity of the polymer obtained was 0.81 dl/g at a concentration of 0.5 g/dl in *N,N*-dimethylacetamide at 30°C.

Preparation of Membranes

4SMI-60 (4g) was dissolved in 20ml of *N*-methyl-2-pyrrolidone (NMP). The solution was filtered and the filtrate was cast on a polypropylene film at room temperature. By evaporating the NMP at 80°C for an hour, the

membrane of 10-20 μm thickness was obtained; this membrane will be called as-cast membrane hereafter.

Thermal treatment of the as-cast membrane was carried out by keeping the membrane at various temperatures under reduced pressure (ca. 0.5 mmHg) for 17 hours.

Extraction of the NMP from the as-cast membrane was carried out by immersing the membrane into acetone for 17 hours. The following thermal treatment was performed in the same manner as that of the as-cast membrane.

Permeability measurement

Permeabilities of H₂ and CO were measured in the same way as that in Chapter 4.

Analysis of Membranes

Densities were measured as described in Chapter 4.

Amount of residual solvent was measured by use of a thermogravimetric analyzer (Shimadzu TG-30). Difference of the sample weight between 160°C and 310°C was measured at a heating rate of 10°C/min in air. The weight loss in this region has no relation to the evaporation of water absorbed in the membrane or decomposition of the polymer, and hence is attributable to the evaporation of the NMP.

Thermomechanical analysis (TMA) was carried out on the films, 1mm wide and 5mm long, with a Shimadzu TMA-30.

Change in length of the samples was measured with the elongation mode under a load of 200mg at a heating rate of 10°C/min in air.

Dynamic viscoelastic property was measured at 110Hz and a heating rate of 2°C/min in air with a Toyo Baldwin Rheovibron DDV-2E.

6-3 Results and Discussion

6-3-1 Thermal Treatment of As-cast Membrane

The as-cast membrane of 4SMI-60, which was dried at 80°C for an hour after the cast, was thermally treated for 17 hours at various temperatures under reduced pressure. Then, permeability coefficients for H₂ and CO (P_{H_2} and P_{CO}) were measured at 30°C. Figure 1 shows changes in P_{H_2} and P_{CO} by the thermal treatment. Regardless of the temperature of thermal treatment, P_{H_2} kept a constant value near 3×10^{-10} cm³·cm/cm²·s·cmHg. On the other hand, P_{CO} decreased from 6.0×10^{-12} to 2.3×10^{-12} cm³·cm/cm²·s·cmHg, when the treatment temperature rose from 30° to 220°C. As a result, P_{H_2}/P_{CO} increased from 50 to 139 as shown in Figure 2.

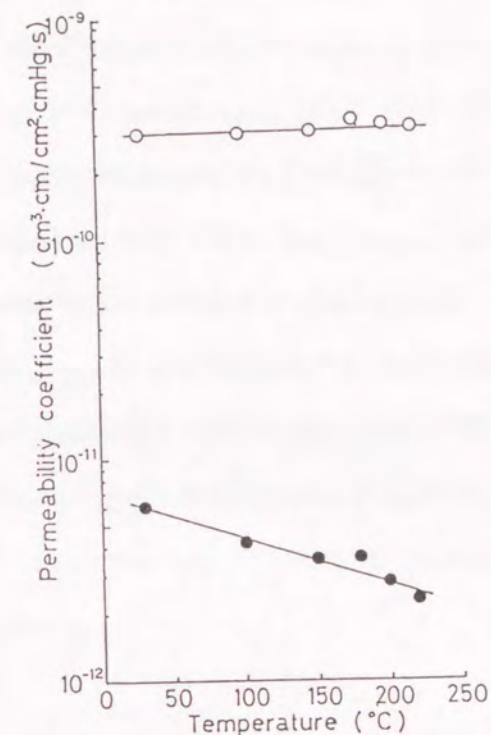


Figure 1. Effect of the thermal treatment on permeability coefficients for H₂ and CO through the 4SMI-60 membrane at 30°C: ○, P_{H_2} ; ●, P_{CO} .

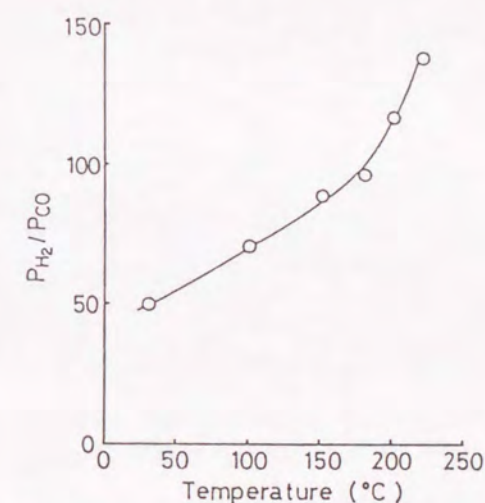


Figure 2. Effect of the thermal treatment on the permeability ratio for H₂ relative to CO of the 4SMI-60 membrane at 30°C.

Figure 3 shows that the apparent diffusion coefficient for CO ($D_{app.CO}$) decreased from 7.3×10^{-9} to 5.5×10^{-10} cm²/s when the thermal treatment temperature changed from 30°C to 220°C. The apparent solubility coefficient for CO ($S_{app.CO}$) calculated by using the relation $P=D \times S$ increased with thermal treatment as shown in Figure 3. Though the reason why $S_{app.CO}$ increased with thermal treatment is not clear from these results, it is concluded that the decrease in P_{CO} was dominated by the decrease in $D_{app.CO}$.

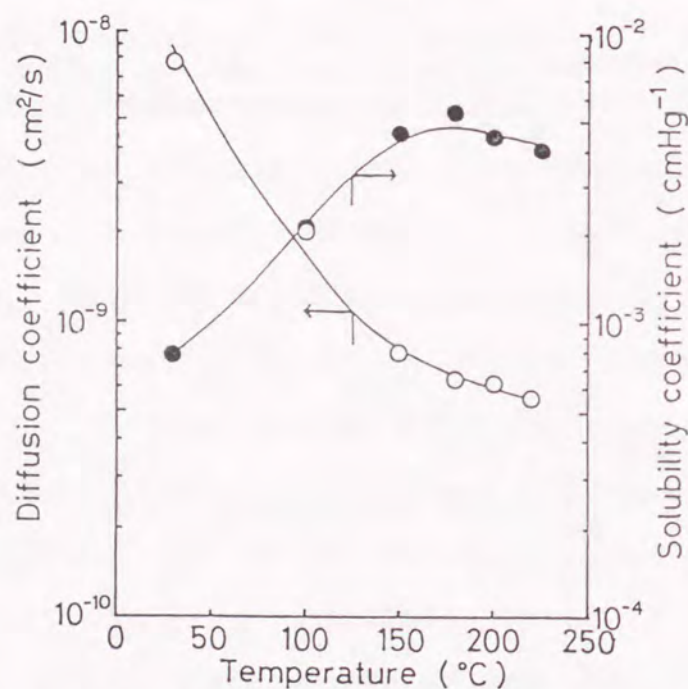


Figure 3. Effect of the thermal treatment on $D_{app.CO}$ and $S_{app.CO}$ of the 4SMI-60 membrane at 30°C.

Packing character of the polymer chains was evaluated from the density measurement of the membranes.

In general, the degree of packing of polymer chains is affected by the crystallinity of a polymer. The X-ray diffraction patterns showed that the poly(sulfone-amide) membranes were amorphous regardless of thermal treatment temperature. Figure 4 shows the X-ray diffraction photograph of the membrane treated at 220°C as an example. Therefore, it is not necessary to consider the influence of crystallinity induced by the thermal treatment on the membrane density.

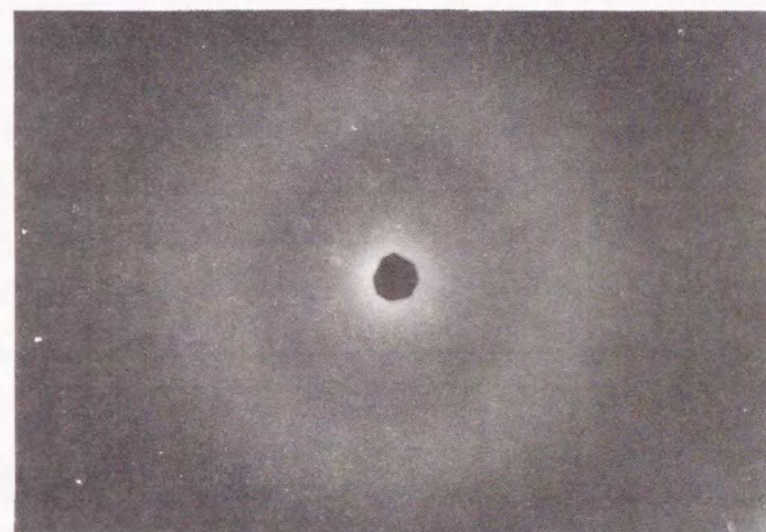


Figure 4. X-ray diffraction pattern of the 4SMI-60 membrane thermally treated at 220°C.

A trace of the residual solvent was detected in each membrane. However, no difference in the amount of residual NMP was detected before and after the gas permeation experiments, and it is concluded that NMP was fixed tightly in the membrane. Some investigators have reported that some solvents, like NMP and hexamethylphosphoramide, form a complex with aromatic polyamides with hydrogen bonding between an amide group of the polyamides and the solvent molecule.¹⁻³

Table I shows the density and amount of residual NMP in the thermally treated membranes. As found in the Table, the increase in density with a rise in temperature of the thermal treatment was affected not only by rear-

Table I. Thermal treatment effects on 4SMI-60 membrane

Thermal treatment temperature	Density ^a	Residual NMP ^b	P_{H_2}/P_{CO^C}
°C	g/cm ³	wt%	
30	1.311	11.8	50
150	1.326	4.3	89
200	1.337	1.2	118
220	1.339	1.1	139

a Measured at 30°C with a density gradient column.

b Determined by thermogravimetric analysis.

c Measured at 30°C.

angement of the polymer chains but also the amount of residual NMP. It is necessary to estimate the influence of solvent in the membrane on the apparent density of membrane.

Here, it is assumed that the density of polymer itself and the density of NMP contribute to the apparent density of membrane independently. The apparent density is expressed by the following equation,

$$\bar{d} = \bar{d}_P \cdot (1 - v_N) + \bar{d}_N \cdot v_N \quad (1)$$

where \bar{d}_P and \bar{d}_N are the densities of the polymer itself and NMP respectively, and v_N is the volume fraction of the NMP in the mixture of polymer and NMP. The following equation also can be written,

$$v_N = \bar{d} \cdot w_N / \bar{d}_N \quad (2)$$

where w_N is the weight fraction of NMP in the mixture. Substituting eq 2 in eq 1 yields the following equation.

$$(\bar{d}_P - \bar{d}_N) \cdot w_N + \bar{d}_N = \bar{d}_P \cdot \bar{d}_N / \bar{d} \quad (3)$$

If \bar{d}_P and \bar{d}_N remain constant without being affected by thermal treatment, a plot of $1/\bar{d}$ vs. w_N gives a straight line. Figure 5 shows a plot of the experimental results. A deviation from the straight line at the low w_N region was considered to be due to the change in \bar{d}_P , because it

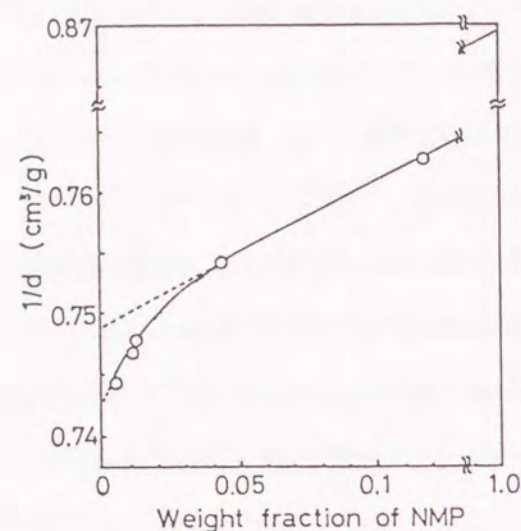


Figure 5. Relation between the apparent density of the 4SMI-60 membrane and the weight fraction of NMP in the membrane.

is unlikely that d_N changes with thermal treatment. When the membrane was thermally treated at a high temperature, the density of the polymer itself became higher and made the slope of this line larger.

From the intercept of the extrapolated line to $w_N = 1$, d_N was determined to be 1.15. This value is not the same as the density value for the liquid state at 30°C.⁴ Assuming the density of NMP to be 1.15 in the membrane, the density of the polymer itself is calculated as shown in Figure 6. In this figure, it is found that the increase of calculated density occurs by the treatment around 180°C or higher temperature. Corresponding to

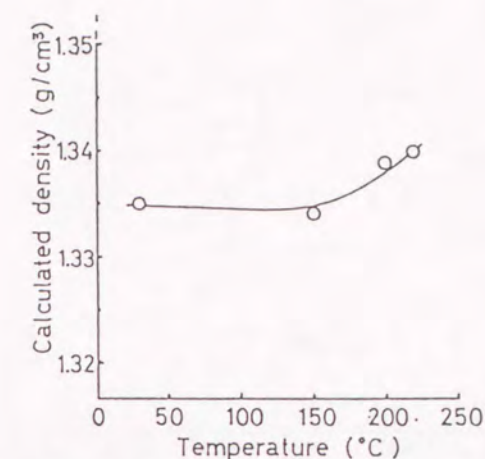


Figure 6. Calculated density of 4SMI-60 itself as a function of the thermal treatment temperature.

this, the treatment in the same temperature region gave a high permselectivity.

In addition to the density measurement, thermomechanical analysis (TMA) and dynamic viscoelasticity were measured to evaluate the structural change in the thermally treated membranes.

Figure 7 shows TMA curves of the membranes thermally treated at various temperatures. In the TMA curves of poly(sulfone-amide), the membrane shrank at first with increasing temperature, and then elongated with further increase in temperature. The elongation temperature did not change significantly with thermal treatment. On the

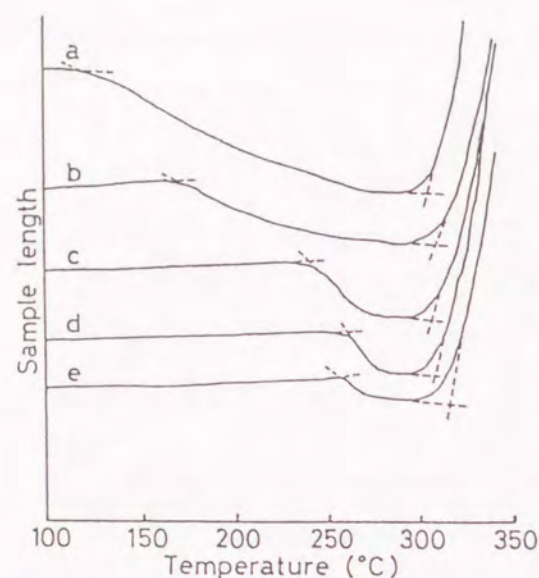


Figure 7. Effect of the thermal treatment on the TMA curves of the 4SMI-60 membranes. The thermal treatment temperatures are: a, 30°C; b, 100°C; c, 150°C; d, 180°C; e, 200°C.

other hand, the shrinking temperature increased with the increase in the thermal treatment temperature.

Figure 8 compares the change in the shrinking temperature with the change in P_{H_2}/P_{CO} by the thermal treatment. When the membrane has a lower shrinking temperature, it is considered that some rearrangement of the polymer chains is possible by further thermal treatment. When the membrane was thermally treated above 180°C, the shrinking temperature reached around 260°C. At the same time, P_{H_2}/P_{CO} became remarkably high. This shows that the membrane having a tightly fixed structure gives high permselectivity.

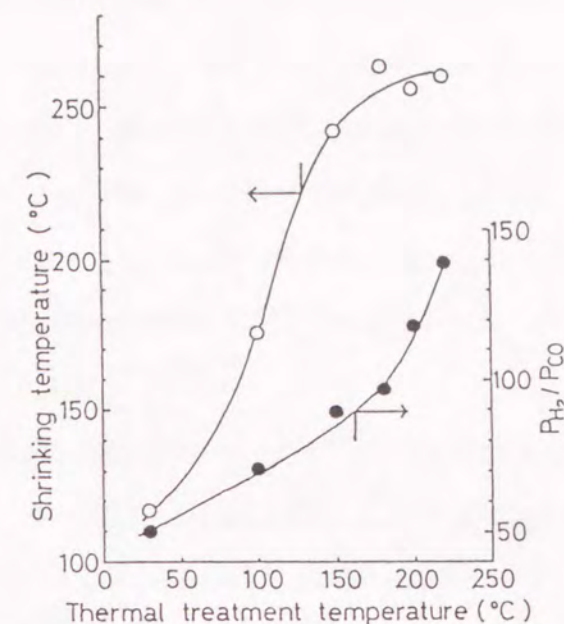


Figure 8. Comparison of the effect of thermal treatment on the shrinking temperature and the permeability ratio for H_2 relative to CO of the 4SMI-60 membrane.

Figure 9 shows $\tan\delta$ change of the membrane by the thermal treatment. The $\tan\delta$ peak around -50°C was independent of the thermal treatment temperature. The $\tan\delta$ peak for glass transition existed above 250°C. There was another peak affected by the thermal treatment between these two peaks. The peak temperature of this transition increased with an increase in the thermal treatment temperature until near 150°C, then, this transition disappeared by the treatment at a higher temperature. The disappearance of this transition suggests that fixing of the membrane structure has progressed.

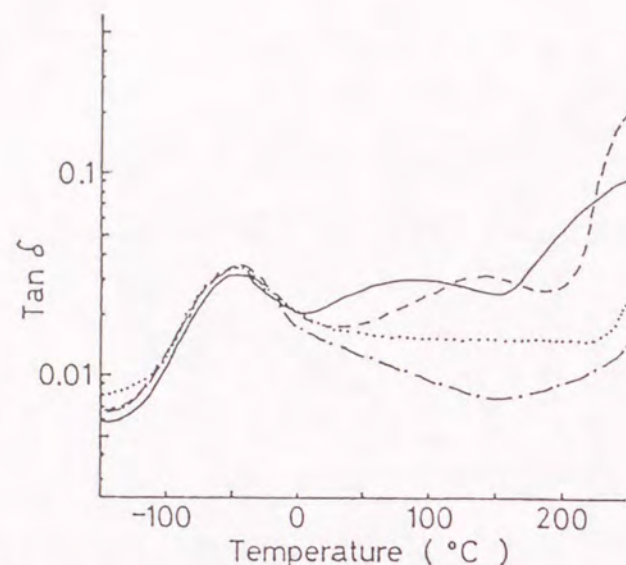


Figure 9. Temperature dependence of $\tan \delta$ for the thermally treated 4SMI-60 membranes. The thermal treatment temperatures are: —, 30°C; ---, 150°C; ····, 200°C; - · -, 220°C.

The effective fixation of polymer chains by the thermal treatment around 200°C was ascertained by dynamic viscoelastic measurement as well as density and TMA measurements. This fixation was related to both the removal of residual NMP and the rearrangement of polymer chains.

6-3-2 Thermal Treatment of Extracted Membrane

Thermal treatment of the as-cast poly(sulfone-amide) membrane brought about removal of the cast solvent and rearrangement of the polymer chains. In order to remove the cast solvent, it is also applicable to immerse a slightly dried membrane into a non-solvent for the polymer.

For this purpose, the as-cast membrane of poly(sulfone-amide) (4SMI-60), which was dried at 80°C for an hour after the cast, was immersed in acetone for 17 hours. Acetone mixes with NMP easily and does not induce swelling of the poly(sulfone-amide) membrane. Therefore, it is an effective non-solvent to extract the NMP from the membrane. The amount of residual NMP decreased from ca. 15wt% to 3.5wt% by this extraction. Then, the thermal treatment under reduced pressure was carried out. Effects of the NMP extraction by acetone and the following thermal treatment on gas permeabilities and some other properties are summarized in Table II.

P_{H_2}/P_{CO} of the membrane after the extraction was 92 and similar to that of the membrane thermally treated at 150°C for 17 hours without extraction, which was 89. The densities and the residual NMP contents were also similar in these two membranes: 1.328 and 3.5wt% for the extracted membrane; 1.326 and 3.5wt% for the thermally treated

Table II. Effects of the extraction of cast solvent and the following thermal treatment on the properties of the poly(sulfone-amide) membrane

Thermal treatment temperature	$P_{H_2}^a$ $\times 10^{10}$	P_{CO}^a $\times 10^{12}$	P_{H_2}/P_{CO}	Density ^b g/cm ³	Residual NMP ^c wt%
r.t.	3.6	3.9	92	1.328	3.5
200°C	4.4	5.0	88	1.335	0.3
220°C	4.5	5.5	82	1.335	0.2

a cm³·cm/cm²·s·cmHg, measured at 30°C.

b Measured at 30°C with a density gradient column.

c Determined by thermogravimetric analysis.

membrane. From these results, it might be considered that the removal of the cast solvent, regardless of extraction or thermal treatment, induced a similar densification of the polymer structure.

The thermal treatment of the extracted membrane, however, gave opposite results from the thermal treatment of the as-cast membrane. As shown in Table II, P_{H_2}/P_{CO} of the extracted membrane decreased in some degree by the following thermal treatment. On the other hand, the thermal treatment of the as-cast membrane increased P_{H_2}/P_{CO} with increasing temperature of the thermal treatment as described in the previous section. This increase was mainly attributed to the decrease in diffusion coef-

ficient for CO ($D_{app.CO}$) as a result of the densification of the membrane structure. In the case of extracted membrane, $D_{app.CO}$ increased with the thermal treatment as illustrated in Figure 10. Although the extraction step caused some densification by removing the NMP, the following thermal treatment reduced the compactness instead of increasing the degree of packing.

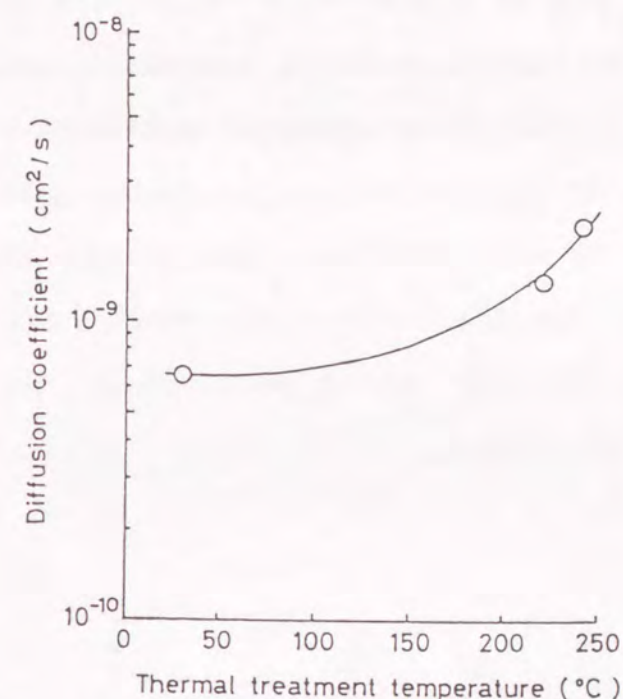


Figure 10. Effect of thermal treatment on the apparent diffusion coefficient of CO for the 4SMI-60 membrane extracted by acetone.

To understand the structural difference between the thermally treated membranes with and without the extraction, the following characterization was carried out.

Figure 11 shows $\tan\delta$ profiles of the extracted membrane with the following thermal treatment. The $\tan\delta$ peaks between the peak around -50°C and the glass transition (263°C) give some information about the effect of thermal treatment. In the case of thermal treatment of the as-cast membrane, increasing the temperature of thermal treatment shifted this peak between the two major transitions to higher temperature region and finally this peak disappeared. Similarly, the corresponding transitions for the extracted membrane disappeared with thermal treatment. The increase in the density with thermal treatment for the extracted membrane (Table II) was also similar to that for the as-cast membrane. No remarkable difference in heat set was detected from these macro-

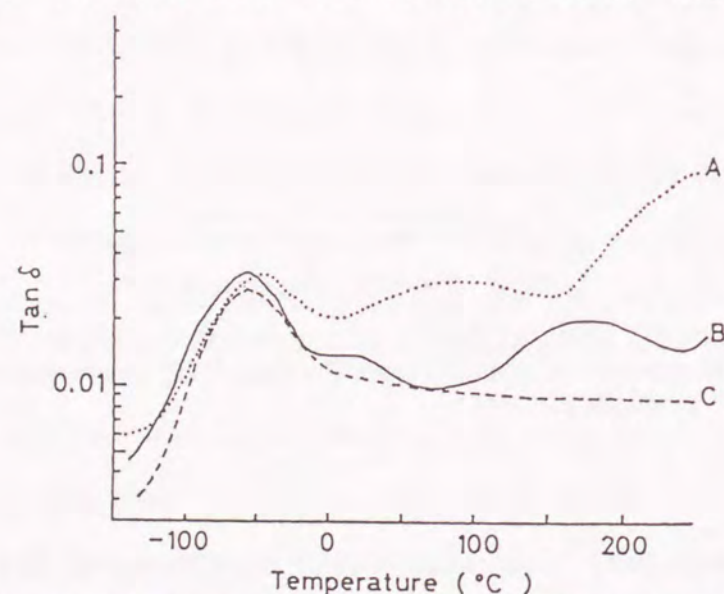


Figure 11. Temperature dependence of $\tan\delta$ for the 4SMI-60 membrane: A, as-cast; B, immersed in acetone for 17 hours; C, thermally treated at 200°C for 17 hours after the extraction.

scopic views.

Some difference in microscopic aspect for these two systems is explained by the results of TMA measurement. As illustrated in Figure 12, the extracted membranes showed two-step elongation on TMA. The first elongation temperature depended on the thermal treatment temperature to some extent, and the second one appeared at almost the same temperature.

As reported in the previous section, the membranes without extractions shrunk at first and then elongated on TMA. This shrinking temperature increased with increas-

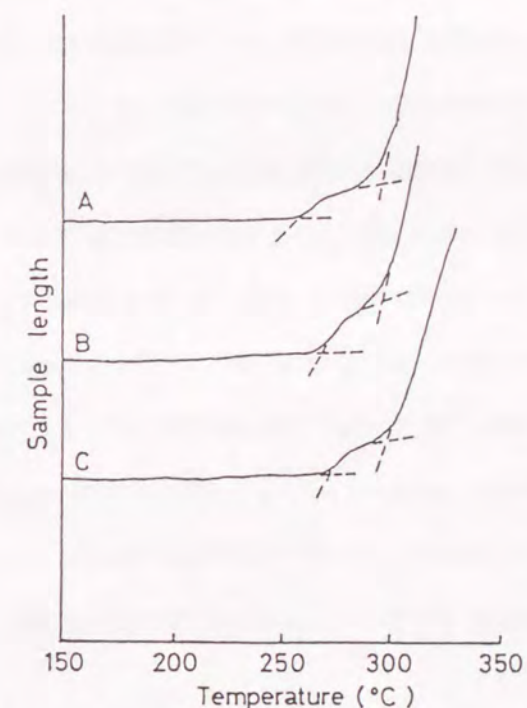


Figure 12. Effect of the thermal treatment on TMA curves of the 4SMI-60 membrane extracted by acetone. The thermal treatment temperature: A, 30°C ; B, 200°C ; C, 220°C .

ing temperature of the thermal treatment. This shrinking phenomenon suggests that the membrane has residual stress in it, and more densification is possible with further thermal treatment at higher temperatures. The extraction itself induced ca. 10% shrinkage of a length of the membrane and removed most of the cast solvent. Therefore, it is considered that there was no shrinkage on TMA because the stress in the membrane had already been removed at the stage of the extraction.

In the case of the as-cast membrane, the residual solvent in the membrane makes the polymer chains rearrange easily at a relatively lower temperature. At the same time, the residual stress seems to contribute to a uniform densification effectively. As the extracted membrane does not have such effects, the densification is probably not uniform in the membrane and increased the defects which accelerate the diffusivity of gas molecules. As a result, P_{H_2} and P_{CO} increased, and P_{H_2}/P_{CO} decreased with the thermal treatment.

As discussed above, it was ascertained that the residual solvent plays an important role to determine the membrane structure in the course of its removal.

6-4 Conclusions

The thermal treatment above ca. 150°C of the as-cast membrane, which contained about 15wt% of NMP, induced removal of the NMP and rearrangement of the polymer chains. On the other hand, the thermal treatment at lower temperature only resulted in the removal of NMP. The rearrangement of the polymer chains contributed to the densification of membrane structure and the increase of permselectivity of H_2 and CO . This structural change was ascertained by density measurement, thermomechanical analysis and dynamic viscoelastic measurement.

When the residual NMP in the membrane was removed by extraction, the residual stress was also eliminated. As a result, the following thermal treatment induced the formation of some defects, which accelerated the gas diffusivity, in the membrane.

Based on these results, advantages in the thermal treatment for the as-cast membrane were explained as follows: (1) the influence of the residual solvent which lowered the temperature possible for the polymer-chain rearrangement, (2) the effect of residual stress which contributed to the uniform densification of membrane.

References

1. T.Takahashi, T.Yamamoto and I.Tsujimoto, *J. Macromol. Sci., Phys.*, B16, 539(1979)
2. S.Minami, H.Kakida and J.Nakauchi, *JP Kokai Tokkyo Koho* 52-13545, 52-84285, and 52-98764
3. V.V.Kochervinsky, V.M.Zagainov, V.G.Sokolov and Y.V. Zelenov, *J. Polym. Sci., Polym. Chem. Ed.*, 19, 1197(1981)
4. The density of NMP at 25°C is 1.027 (from a catalog of Mitsubishi Chemical Industries, Ltd.)

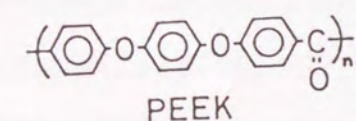
Chapter-7

Effects of Polymer Structure and Thermal Treatment on Gas Permeability of Poly(ether ketone)s

7-1 Introduction

In previous chapters, gas permeability of the poly(sulfone-amide) membranes was studied. In the case of poly(sulfone-amide), as content of amide linkages in the polymer chain increased, the polymer became stiffer and gas permeation was restricted. Intermolecular hydrogen bonding might play some role in this effect. When the poly(sulfone-amide)s had the same amide-bond concentration, an increase in the *meta*-catenation ratio relative to the *para*-catenation induced the more compact packing of the polymer chains and gas diffusivity decreased. This catenation effect has been also reported for other polymers recently.¹⁻⁶ In order to design H₂/CO separation membrane of poly(sulfone-amide), a suitable polymer structure should be selected by considering these two effects.

In this chapter, concern was paid to gas permeability of poly(ether ketone) copolymers. Poly(ether ketone)s such as PEEK are well known as a high-performance semi-



crystalline engineering plastics with excellent heat stability and solvent resistance. However, PEEK dissolves only in few solvents such as sulfuric acid, and it

is hard to obtain a uniform film by the cast method. Therefore, reports about gas permeability of PEEK films are very few. There are some reports for gas permeability of modified poly(ether ketone)s, which are soluble in organic solvents, with cardo substituents^{7,8} or fluorine-containing structure.⁹

The poly(ether ketone)s described in this paper have simple structures consisting of ether, carbonyl and phenylene groups. These polymers were prepared by Friedel-Crafts acylation between diphenyl ether and mixed acid chloride comprising terephthaloyl chloride and isophthaloyl chloride. Most of these copolymers dissolved in hexafluoro-2-propanol and their films could be obtained by the cast method.

As structural difference in the poly(ether ketone)s exists only in the *meta/para* ratio, the catenation effect was studied and compared with that found in the poly(sulfone-amide)s. In addition, another effect induced by the semi-crystalline characteristics of poly(ether ketone)s was expected. Structural change and permeability change in the poly(ether ketone) films by thermal treatment were also examined, and compared with that of the poly(sulfone-amide)s.

7-2 Experimental

Materials

Isophthaloyl chloride (IPC), terephthaloyl chloride (TPC), obtained from Mitsubishi Gas Chemical Co., Inc., and aluminum chloride (Nacalai Tesque, EP.) were crushed to powders under nitrogen atmosphere. 1,1,1,3,3,3-hexafluoro-2-propanol (HFIP)(Nacalai Tesque, GR.) was purified by distillation. Diphenyl ether and 1,2-dichloroethane were purchased from Nacalai Tesque as GR. and used without further purification.

Polymerization

Polymerization procedure for the poly(ether ketone) from diphenyl ether and isophthaloyl chloride is described below as a typical example.

In a 300ml 4-necked flask, equipped with a mechanical stirrer, a nitrogen inlet and a thermometer, were placed diphenyl ether(12.22g, 0.0718mole), IPC(14.58g, 0.0718mole) and 200ml of dichloroethane. This solution was cooled below 5°C in an ice bath and then AlCl_3 (24.96g, 0.187mole) was added. After the reaction mixture was stirred for 2 hours in the ice bath, the polymerization was continued for 16 hours at room temperature. The dichloroethane was decanted from the reaction

mixture, and methanol was mixed with the product. The polymer obtained was washed with 10% HCl aqueous solution twice and pure water several times by use of a blender, and then dried at 150°C for 17 hours under reduced pressure.

The other polymers were prepared with the same method except using the mixed monomers with several ratios of IPC and TPC.

Film Preparation

The polymer(500mg) was dissolved in 5ml of HFIP and filtered. The solution was cast on a glass plate, and the solvent was evaporated by the irradiation with an infrared lamp. The film obtained was immersed in acetone more than one day to extract the cast solvent, and dried at 120°C for 17 hours in a vacuum oven.

Thermal treatment of the poly(ether ketone) films was carried out at 195°C in the vacuum oven.

Permeability measurement

The permeabilities of H₂, O₂, CO and N₂ were measured in the same way described in chapter 4. Gas samples of purity exceeding 99.9% were used.

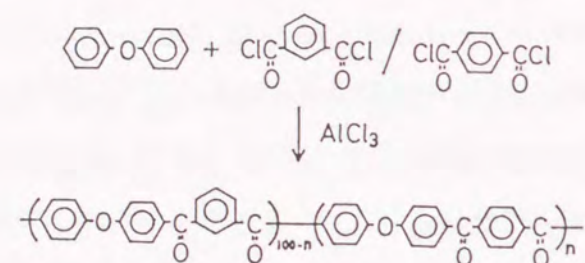
Characterization

Inherent viscosities of the polymers were measured at a concentration of 0.5g/dl in 95% sulfuric acid at 30°C. DSC measurement was carried out on a Perkin-Elmer DSC-1B with 10mg sample at a heating rate of 20°C/min under argon flow. Thermogravimetric analysis (TGA) was performed on a Shimadzu TG-30 with 3-6mg sample at a heating rate of 10°C/min in air. Densities of the membranes were measured by use of a density gradient column which consisted of n-heptane and carbon tetrachloride at 30°C. Wide angle X-ray scattering was conducted on a Rigaku X-ray diffractometer with nickel-filtered CuK α radiation (40KV, 100mA).

7-3 Results and Discussion

7-3-1 Polymer Structure and Gas Permeability of Poly(ether ketone)s

Synthesis of poly(ether ketone) by Friedel-Crafts acylation was discussed in chapter 2. In this chapter, the poly(ether ketone)s from diphenyl ether and the mixed acid chloride comprising IPC and TPC were prepared as shown below.



The results of the preparation and characterization are shown in Tables I and II. Each polymerization gave the almost quantitative yield and the inherent viscosity more than 0.8 dl/g. The glass transition temperature increased monotonously from 156 to 174°C with an increase in the content of TPC unit. EI and ET showed clear melting points at 274 and 378°C, respectively. Copolymerization decreased and broadened the melting point. All the polymers except ET easily dissolved in HFIP.

Table I. Preparation of poly(ether ketone)s

Polymer	Monomer Ratio		Yield (%)	η_{inh}^a (dl/g)
	IPC	TPC		
EI	100	0	97	0.87
EIT25	75	25	94	0.94
EIT50	50	50	94	0.80
EIT75	25	75	95	0.96
ET	0	100	94	0.92

^aInherent viscosity measured at a concentration of 0.5g/dl in H₂SO₄ at 30°C.

Table II. Properties of poly(ether ketone)s

Polymer	T _g ^a (°C)	T _m ^a (°C)	TGA ^b (°C)	Solubility ^c
EI	156	274	505	soluble
EIT25	160	227	492	soluble
EIT50	161	232	502	soluble
EIT75	168	333	482	soluble
ET	174	378	492	insoluble

^aGlass transition and melting temperatures determined by DSC in argon with a heating rate of 20°C/min.

^b5% weight loss temperature measured by thermogravimetric analysis in air with a heating rate of 10°C/min.

^cSolubility in HFIP at room temperature.

The films of EI, EIT25, EIT50, and EIT75 were prepared by the cast method. The films prepared were immersed in acetone more than one day to extract the HFIP completely. The permeability coefficients P for H_2 , O_2 , CO and N_2 at 30°C are illustrated in Figure 1. P_{H_2} was between 2.5×10^{-10} and $2.9 \times 10^{-10} \text{ cm}^3 \cdot \text{cm} / \text{cm}^2 \cdot \text{s} \cdot \text{cmHg}$, and no remarkable dependence on the polymer composition was observed. On the other hand, in the case of larger molecules, O_2 , CO and N_2 , the permeability coefficients

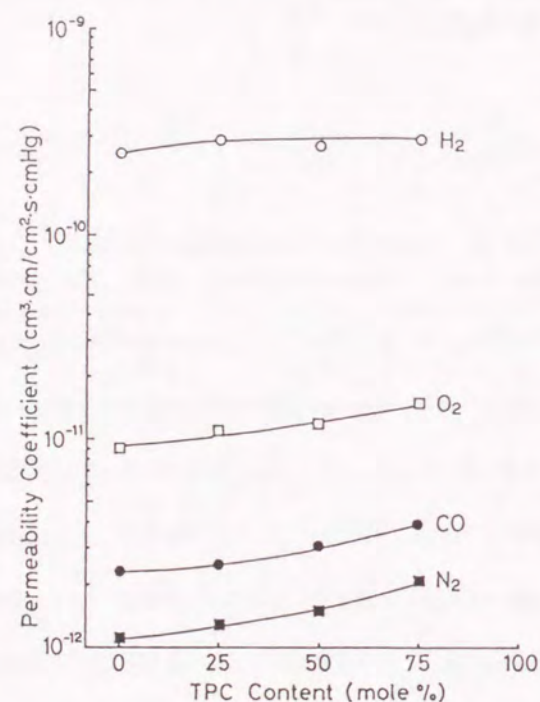


Figure 1. Correlation between the chemical composition of as-cast films of poly(ether ketone) copolymers and the gas permeability coefficients for H_2 , O_2 , CO and N_2 at 30°C .

increased with an increase in the TPC content; for example, P_{N_2} increased almost twice from 1.1×10^{-12} at 0 TPC mole% to 2.1×10^{-12} at 75 TPC mole%.

The apparent diffusion coefficients D_{app} for O_2 are plotted against the TPC content in Figure 2(a). D_{app, O_2} increased with the increase in the TPC content. In Figure 2(b) are shown the apparent solubility coefficients S_{app} for O_2 , which were calculated by using the formula $S = P/D$. Though measurements are limited to only one upstream pressure, the solubility coefficient seems to be independent of the TPC content. Therefore, it is

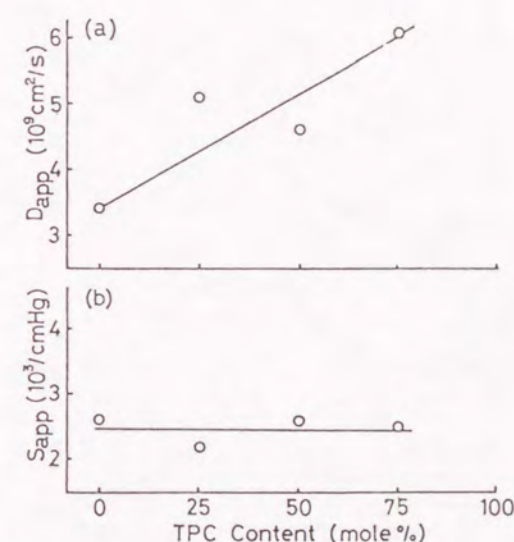


Figure 2. Effect of the chemical composition on the apparent diffusion coefficient (a) and the apparent solubility coefficient (b) of the as-cast poly(ether ketone) films for O_2 .

considered that the increase in the permeability with increasing TPC content was caused by the diffusivity change. This tendency is consistent with the results of poly(sulfone-amide)s described in the previous chapters; the increase in the ratio of *p*-catenation content relative to *m*-catenation made the chain packing less compact and the gas diffusivity higher.

To elucidate a crystallinity effect on the gas permeability, wide angle X-ray scattering measurement (WAXS) was carried out. The X-ray diffractograms of the copolymers are shown in Figure 3. The diffraction peaks

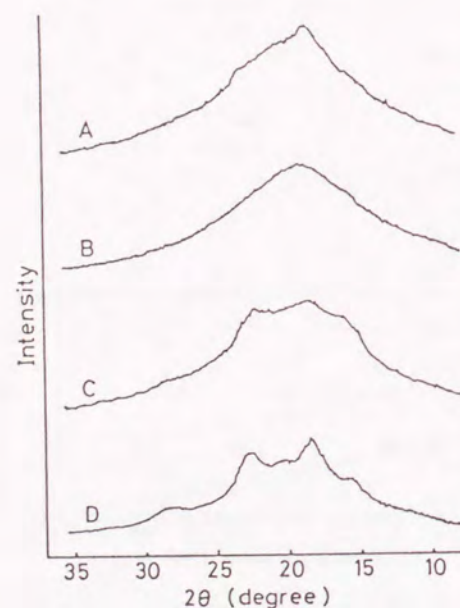


Figure 3. X-ray diffractograms of the poly(ether ketone) films without thermal treatment: A, EI; B, EIT25; C, EIT50; D, EIT75.

from crystalline structure were observed for the EIT75 film (D). For the other polymer films, however, no apparent crystalline peak was observed, and the films are considered to be almost amorphous. Though EIT75 had a certain extent of crystalline area in which a gas molecule hardly permeate^{10,11}, no influence of the crystallinity was observed in the results of permeability measurement. In the amorphous region of EIT75, the polymer chains would have less compact packing to offset the crystallinity effect. There also may exist some fine defects, which are in favor of high gas diffusivity, in the amorphous region of EIT75.

7-3-2 Gas Permeability of the Thermally Treated Films

The poly(ether ketone) films were thermally treated at 195°C under reduced pressure, above their glass transition temperatures. The permeability coefficients of the films after 1-hour treatment for the four gases are illustrated in Figure 4. In all the polymers except EIT25, the permeability coefficients for each gas decreased by 10-60% with the thermal treatment. For EIT25 films, P_{H_2} showed no change, and the permeabilities of the other gases increased about 10-45% with the thermal treatment.

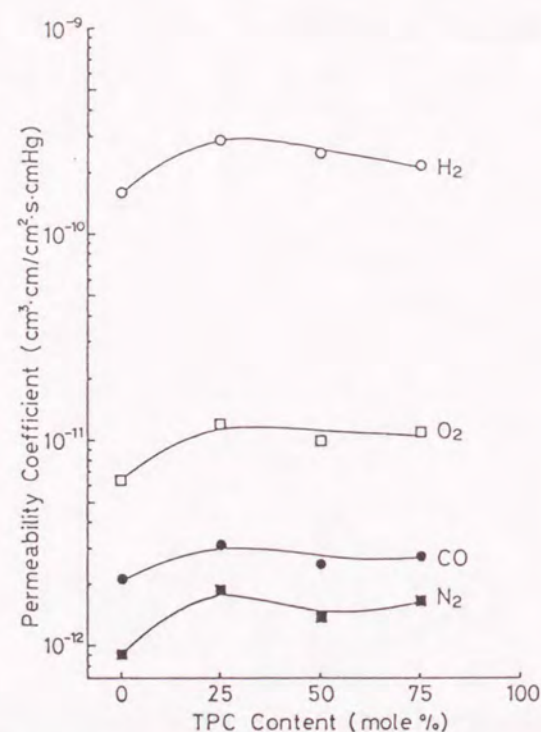


Figure 4. Correlation between the chemical composition of poly(ether ketone) copolymers thermally treated 1 hour and the gas permeability coefficients for H_2 , O_2 , CO and N_2 at 30°C.

The X-ray diffraction patterns of the films after 1-hour treatment are shown in Figure 5. The crystalline peaks were observed clearly in EI (A) and EIT75 (D), and to some extent in EIT50 (C). On the other hand, EIT25 (B) still showed a broad amorphous pattern. After further thermal treatment for 5 hours, no change was detected in EI, EIT25, and EIT75 any more, and the crystalline peaks became higher in EIT50 as shown in Figure 6. These results indicate the fast crystallization in EI and EIT75, the slow crystallization in EIT50, and no crystallization in EIT25. The crystallization behavior was also confirmed with the density measurement as shown in Table III. The densities of the films except EIT25 increased with the thermal treatment. From these evaluations, it is considered that the permeability change by the thermal treatment was clearly related to the crystallization.

Table III. Density of the poly(ether ketone) films

Polymer	Thermal Treatment		
	none	1hr	6hr
EI	1.27	1.30	1.30
EIT25	1.28	1.28	1.28
EIT50	1.27	1.29	1.30
EIT75	1.29	1.31	1.31

* Density measurement was performed at 30°C.

** Thermal treatment was carried out at 195°C under vacuum.

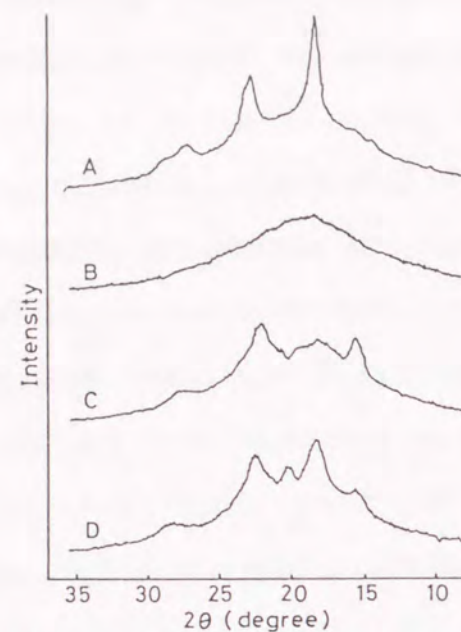


Figure 5. X-ray diffractograms of the poly(ether ketone) films after 1-hour thermal treatment at 195°C: A, EI; B, EIT25; C, EIT50; D, EIT75.

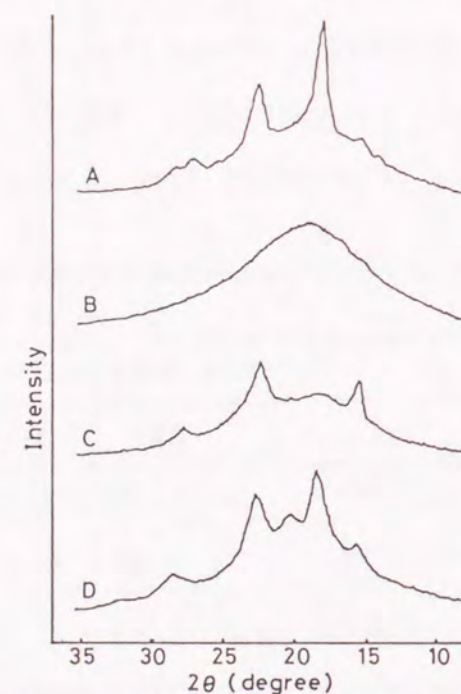


Figure 6. X-ray diffractograms of the poly(ether ketone) films after 6-hour thermal treatment at 195°C: A, EI; B, EIT25; C, EIT50; D, EIT75.

The apparent diffusivity change of O_2 by the thermal treatment is shown in Figure 7(a). The diffusion coefficients for EI, EIT25 and EIT50 increased slightly at the early stage of the thermal treatment. Although the amorphous region in EI and EIT50, which allows gas diffusion, became smaller with the growth of crystalline region by the thermal treatment, the apparent gas diffusivity did not decrease. This is considered to be due to the creation of some fine defects in the amorphous region by the thermal treatment. In the case of EIT75, the existence of defects before the thermal treatment is supposed, and further defect formation may be small. Similar effect was also observed in the thermal treatment

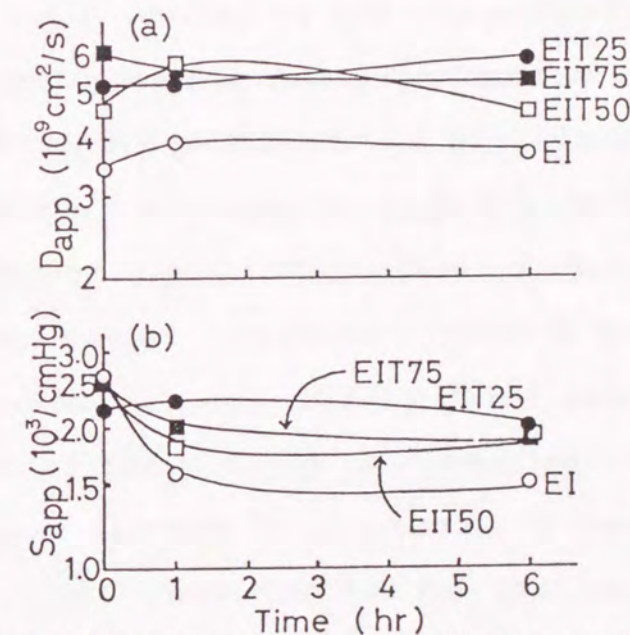


Figure 7. Change of the apparent diffusion coefficient (a) and the apparent solubility coefficient (b) for O_2 by the thermal treatment at 195°C.

of the extracted poly(sulfone-amide) films as discussed in chapter 6. It seems difficult to bring about homogeneous densification in the amorphous region, which is effective to reduce gas diffusion, by thermal treatment without containing solvent.

A decrease in apparent solubility coefficients for O_2 was found in EI, EIT50, and EIT75 as shown in Figure 7 (b). This is consistent with the fact that a gas hardly dissolves into a crystalline region. No crystallization occurred in EIT25, and no remarkable solubility change was detected. The permeability change in the poly(ether ketone) films by the thermal treatment seems to be dominated by the solubility change rather than the diffusivity change.

From the discussion mentioned above, the decrease in the gas permeability by the thermal treatment is concluded to be caused by the increase in the degree of crystallinity of the semi-crystalline poly(ether ketone)s induced by the thermal treatment. In the case of amorphous poly(ether ketone), the homogeneous densification due to the rearrangement of polymer chains seems not to be easy without the presence of solvent molecules, and the gas permeability did not decrease.

7-4 Conclusions

Gas permeability of the as-cast films of poly(ether ketone) copolymers made from diphenyl ether and the mixed acid chloride comprising IPC and TPC was influenced by the chain-packing character with the catenation effect. An increase in the *m*-catenation ratio relative to *p*-catenation made chain packing more compact, and reduced the gas diffusivity. Difference in crystallinity among the polymers was too small to exhibit apparent effect on the gas permeability.

The permeability change of the poly(ether ketone) films by thermal treatment was interpreted to be due to the decrease in the content of the amorphous region, in which gases can permeate, by the thermal crystallization. Densification in the amorphous region was not observed, and the diffusivity increase was explained in terms of the formation of small defects in it.

References

1. G.F.Sykes and A.K.St.Clair, *J. Appl. Polym. Sci.*, 32, 3725(1986)
2. S.A.Stern, Y.Mi, H.Yamamoto and A.K.St.Clair, *J. Polym. Sci., Polym. Phys. Ed.*, 27, 1887(1989)
3. F.P.Sheu and R.T.Chern, *J. Polym. Sci., Polym. Phys. Ed.*, 27, 1121(1989)
4. K.Tanaka, H.Kita, K.Okamoto, A.Nakamura and Y.Kusuki, *Polym. J.*, 22, 381(1990)
5. K.Tanaka, H.Kita and K.Okamoto, *Kobunshi Ronbunshu*, 47, 945(1990)
6. R.E.Kesting, A.K.Fritzsche, M.K.Murphy, C.A.Cruse, A.C.Handermann, R.F.Malon and M.D.Moore, *J. Appl. Polym. Sci.*, 40, 1557(1990)
7. W.T.Chen and J.Xu, *J. Membr. Sci.*, 53, 203(1990)
8. I.Engelmann, J.D.Schultze, M.Bohning and J.Springer, *Makromol. Chem., Macromol. Symp.*, 50, 79(1991)
9. J.M.Mohr, D.R.Paul, G.L.Tullos and P.E.Cassidy, *Polymer*, 32, 2387(1991)
10. A.S.Michaels and R.B.Parker, Jr, *J. Polym. Sci.*, 41, 53(1959)
11. A.S.Michaels and H.J.Bixler, *J. Polym. Sci.*, 50, 393(1961)

Summary

Whole aromatic polyamides were synthesized from four new phenylated aromatic diamines. By using the para-oriented diamine in which the phenyl groups were placed in the unsymmetrical positions, a rigid rod-like polyamide soluble in *N*-methyl-2-pyrrolidone was obtained, and showed a liquid crystalline character.

The effects of reaction conditions on preparation of poly(ether ketone) via Friedel-Crafts acylation were investigated. Although the polymer precipitated out as a complex with the catalyst, the molecular weight of the polymer increased even after the formation of precipitates. Moreover, the optimum conditions to obtain a high molecular weight polymer were clarified.

Polyphosphoric acid was examined as a polymerization medium for polyimides, and the polyimide was successfully synthesized from 4,4'-diaminodiphenyl ether and 3,3',4,4'-biphenyltetracarboxylic dianhydride in Polyphosphoric acid. By using this imide-formation reaction, poly(imide-benzoxazole) solution in polyphosphoric acid was obtained by one-pot polymerization.

The permeabilities of hydrogen and carbon monoxide through poly(sulfone-amide) membranes were mainly dominated by the degree of packing of the polymer chains. It

was found that the degree of packing for the poly(sulfone-amide) copolymers was increased with increasing ratio of *m*-phenylene content to *p*-phenylene content in the polymer backbone. On the basis of these results, a poly(sulfone-amide) membrane which showed extremely high H₂/CO permselectivity was obtained.

It was found that the residual cast-solvent in the poly(sulfone-amide) membranes played an important role for the densification of membranes during thermal treatment; the residual solvent made the rearrangement of polymer chains possible at a relatively low temperature to induce uniform densification of the membrane. On the other hand, thermal treatment of the membrane without residual solvent induced the formation of some defects in the membrane, and then the gas permselectivity decreased.

Gas permeabilities of poly(ether ketone) copolymers were also controlled by the packing character of the polymer chains, which was influenced by the ratio of *m*-phenylene content to *p*-phenylene content in the polymer backbone. The permeability change of the poly(ether ketone) membranes by thermal treatment was explained by the decrease in the content of amorphous region, where gases can permeate, by the thermal crystallization.

Conclusions

Aromatic condensation polymers are well-known to be useful as engineering plastics owing to their superior thermal stability, chemical resistance, and mechanical behavior. However, these properties also make it difficult to process and fabricate the polymers. From these points of view, a number of researches have been reported to enhance the solubility of aromatic polymers. In this thesis, research on the preparation of soluble aromatic condensation polymers based on the following three points were performed, and several new findings were obtained. (1) To understand the relationships between polymer structure and solubility, new series of aromatic polyamides with phenyl substituents were prepared. Among them, a new rigid rod-like aromatic polyamide, which was soluble in an organic solvent, with a liquid crystalline character was obtained. (2) To clarify optimum polymerization conditions for a potentially soluble polymer which has difficulties in the polymerization, the preparation of poly(ether ketone) via Friedel-Crafts acylation was studied. The preparation of various types of soluble poly(ether ketone)s with high enough molecular weight is considered to be possible by using the polymerization conditions obtained. (3) To find out a new solvent for a polymer which is insoluble in most of solvents, poly-

phosphoric acid was examined as a polymerization medium for polyimides. Polyphosphoric acid was found to be suitable for imide-ring formation, and accordingly poly(imide-benzoxazole) was obtained as a homogeneous solution by this method.

Gas separation membranes for the mixture of hydrogen and carbon monoxide were obtained from soluble aromatic polyamides and poly(ether ketone)s. Key factors in polymer structure to determine the gas permeability were clarified by using series of copolymers in which the polymer structure was systematically altered. On the basis of the information obtained, a membrane with extremely high gas permselectivity was obtained. It was also found that residual solvent in the membrane played an important role to control the membrane structure in the process of membrane formation.

As described above, several new soluble aromatic condensation polymers and highly permselective hydrogen-gas separation membranes were obtained. These findings are also expected to be utilized for the molecular design of new aromatic condensation polymers which have superior properties.

List of Publications

1. Synthesis and Characterization of Aromatic Polyamides Derived from New Phenylated Aromatic Diamines
Y.Sakaguchi and F.W.Harris, *Polym. J.*, 24(1992), in press
2. Synthesis of Poly(ether ketone) by Friedel-Crafts Acylation: Effects of Reaction Conditions
Y.Sakaguchi, M.Tokai and Y.Kato, *Polymer*, under submission
3. Synthesis of Polyimide and Poly(imide-benzoxazole) in Polyphosphoric Acid
Y.Sakaguchi and Y.Kato, *J. Polym. Sci., Polym. Chem. Ed.*, under submission
4. Separation of H₂ and CO through Poly(sulfone-amide) Membranes
Y.Sakaguchi, H.Kawada and Y.Kato, *Kobunshi Ronbunshu*, 43, 755(1986)
5. Separation of H₂ and CO through Poly(sulfone-amide) Membranes II. Highly Permselective Membranes Containing Bis(3-aminophenyl)sulfone as a Diamine Component
Y.Sakaguchi, M.Tokai, H.Kawada and Y.Kato, *Polym. J.*, 20, 365(1988)
6. Separation of H₂ and CO through Poly(sulfone-amide) Membranes III. Changes of Gas Permeability and Membrane Structure in the Process of Solvent Removal
Y.Sakaguchi, M.Tokai, H.Kawada and Y.Kato, *Polym. J.*, 20,

785(1988)

7. Separation of H₂ and CO through Poly(sulfone-amide) Membranes IV. Effects of Extraction of Cast Solvent and Following Thermal Treatment

Y.Sakaguchi, M.Tokai, H.Kawada and Y.Kato, *Polym. J.*, 23, 155(1991)

8. Separation of H₂ and CO through Poly(sulfone-amide) Membranes V. Polymer Structure and Gas Permeability

Y.Sakaguchi, M.Tokai, H.Kawada and Y.Kato, *Polym. J.*, 24, 703(1992)

9. Effects of Polymer Structure and Thermal Treatment on Gas Permeability of Poly(ether ketone)s

Y.Sakaguchi, *Polymer*, in press

